PON Ricerca e Innovazione 2014- 2020
Unione Europea
Ministero dell'Istruzione, dell'Università e della Ricerca

UNIVERSITÀ DEGLI STUDI DI NAPOLI FEDERICO II

PhD Thesis in Industrial Products and Process Engineering

Dynamic Topographic Pattern On Photoswitchable Azobenzene-Substrates To Study Cell Behavior

Eng. Lucia Rossano

Supervisor
Prof. Dr. Paolo A. Netti

Advisors
Dr. Silvia Cavalli
Prof. Dr. Maurizio Ventre

Coordinator
Prof. Dr. Giuseppe Mensitieri

November 2014 – November 2017

DYNAMIC TOPOGRAPHIC PATTERN ON PHOTOSWITCHABLE AZOBENZENE-SUBSTRATES TO STUDY CELL BEHAVIOR

A THESIS SUBMITTED IN PARTIAL FULFILLMENT OF THE REQUIREMENT FOR THE DEGREE OF DOCTOR OF PHILOSOPHY IN
INDUSTRIAL PRODUCTS AND PROCESS ENGINEERING

AUTHOR
Eng. Lucia Rossano

SUPERVISOR
Prof. Dr. Paolo A. Netti

ADVISORS
Dr. Silvia Cavalli
Prof. Dr. Maurizio Ventre

COORDINATOR
Prof. Dr. Giuseppe Mensitieri

Table of Contents

Topic of thesis

The aim of my thesis is to produce and characterize a new class of cell-instructive materials, also known as CIMs, able to change their topographic features in a dynamic manner. *In vivo,* the interplay between cells and surrounding environment is dynamic, in fact, the cells are able to integrate and react to several topographic signals, which continuously change their features in time. For this reason, there has recently been significant attention on new "dynamic" biomaterials that allow mimicking the natural extracellular remodeling. In this context, "light responsive materials" have emerged as powerful tools for cell studies as well as promising for biomedical applications. In detail, the azobenzene-containing polymers can be used to fabricate dynamic-switchable supports for cell culture. Azobenzene molecules can be optically isomerized with light at excitation wavelength and this isomerization induces a unique and remarkable surface mass transport phenomenon on a micrometer and sub-micrometer length scale. The single laser beam of confocal microscope set-up enables a precise spatial and temporal control of the mass migration process by guiding the laser beam switching and position. The polarized light and the proper wavelength lead the isomerization of the azobenzene molecules and the consequent inscription of topographic features on the azopolymer film.

In this thesis, we evaluated the cell response to dynamic topographic features embossed on poly Disperse Red 1 methacrylate-containing films (pDR1m) films. A real-time photopatterning of azofilms was conducted, revealing that cells could sense dynamic topographic changes and spontaneously adapted to a new environment by remodeling their cytoskeleton. Initially, we embossed linear and circular patterns on azofilms in order to evaluate cell behavior in real-time. The fibroblast cells reacted to such "dynamic" topographies, by modifying their morphology and orientation in time. Finally, the real-time modulation of topographies embossed on cell-populated azofilms revealed a variation of Young

modulus of fibroblast cells and a remodeling focal adhesions (FAs). This innovative technique allowed, for the first time, the evaluation of cell properties in response to the spatio-temporal manipulation of topographic cues and taken together, these results underline the possibility to use azobenzene-based platforms as dynamic cell-instructive materials.

Chapter 1

Introduction.*

Abstract. Cell-instructive materials (CIMs) are biomaterials programmed to direct and evaluate the interactions between cells and the surrounding environment. The topographic features of a particular subset of polymeric biomaterials - namely light-responsive azopolymers - can be modulated via light to impart complex commands or instructions to cells in order to guide various aspects of their behavior and to unravel the mechanisms governing the crosstalk between cell membrane and material surface. These light-controlled systems are able to induce programmed changes of cell behavior in time and space, mimicking the spatio-temporal dynamic feature of the *in vitro* extracellular environment. In this Chapter, the main elements of cell-material interactions are reviewed, together with the applications of biomaterials as a cell culture platform. The influence of topographic patterns on cell response has been investigated, focalizing the attention on the limitation of proposed static substrates and exploring a new class of dynamic cell culture platform upon which topographic signals can be presented on-demand using light.

*This Chapter is a part of a review article in preparation: L. Rossano, M. Ventre, S. Cavalli, and P. A. Netti: “Dynamic topographic pattern on photoswitchable azobenzene-substrates to study cell behavior”.

1.1 Synthetic Biomaterials

Tissue engineering combines the principles and the methods of the life sciences with those of engineering to elucidate fundamental understanding of structure-function relationship in tissues, to develop materials and methods to repair damage or diseased tissue and to create entire tissue replacements. A crucial mainstay of tissue engineering are biomaterials that direct cellular behavior and function by mimicking the regulatory characteristics of natural extracellular matrices (ECMs) and cell-ECM interactions, both for therapeutic applications and basic biological studies.[1] The guidance provided by biomaterials may facilitate restoration of structure and function of damaged or dysfunctional tissues, both in cell-based therapies, such as those where carriers deliver transplanted cells or matrices induce morphogenesis in bioengineered tissues constructed *ex vivo* and in other therapies, such as those where materials induce ingrowth and differentiation of cells from healthy residual tissues *in situ*.[2] The principal biomaterial application have been categorized as conducting or guiding a normal biological response,[3] inducing a supernormal biological response,[1] or blocking a naturally occurring, but undesirable, biological phenomenon.[4] Although considerable progress has already been made, critical problems in biocompatibility, mechanical properties, degradation and numerous other areas still remain.[2] At the moment, scientists are creating new materials including those with improved biocompatibility, stealth properties, responsiveness (smart materials), specificity and other critical properties. The current biomaterials were limited to modeling static environments and lacked the spatio-temporal dynamic properties relevant for complex tissue processes.[5] For this purpose, modern biomaterials science is characterized by a growing emphasis on identification of specific design parameters that are critical to better the performance of biomaterials and by a growing appreciation of the need to integrate biomaterials design with new insights emerging from studies of cell-matrix interactions, cellular signaling processes and developmental and systems

biology.[6] Ongoing challenges remain in controlling the dynamics and spatio-temporal presentation of multiple signals in order to mimic the natural cell-extracellular environment interactions.[2]

1.2 Cell-Material Interaction

Numerous biochemical events, ultimately affecting various aspects of cell functions and fate, are triggered and regulated by the cell interaction with the ECM.[7] In brief, a highly dynamic and complex array of biophysical and biochemical signals, transmitted from the outside of a cell by various cell surface receptors and integrated by intracellular signaling pathways, converge to regulate gene expression and ultimately establish cell phenotype.[2] Thus, the ultimate decision of a cell to differentiate, proliferate, migrate, adhere or perform other specific functions is a coordinated response of the molecular interactions with these ECM effectors. The flow of information between cells and their ECM is highly bidirectional[2] and the primary subcellular complex that mediate the regulatory effects of extracellular environment on cell behavior are the focal adhesions (FAs).[8] FAs are dynamic structures involved in the recruitment, interaction and turnover of several molecular components.[9] In detail, the integrins mediate the cell-material interactions, by recognizing specific molecular motifs on the material surfaces. Depending on the density of the adhesive motifs, their distribution and their mechanical compliance, the cell can start to build larger and more stable molecular complexes by involving the cell cytoskeleton assembly to improve the membrane anchorage and to mediate a dynamic material-cytoskeleton crosstalk.[10] Integrins connect the extracellular space to the cytoskeleton; they are not fixed at specific locations in the cell membrane and this mobility lets them to diffuse along the cell membrane and cluster at areas of high ligand density.[11] The cytoskeleton is a dynamic and adaptive structure, it is organized into networks that resist deformation but can reorganize in response to externally applied forces. The

polymerization and depolymerization of actin cytoskeleton filaments generate directed forces that drive changes in cell shape and in the organization of cell components. The assembly of contractile actin-filament bundles, known as stress fibers, is triggered locally when integrins engage their ligands and the actin cytoskeleton is continually assembled and disassembled in response to the local activity of signaling systems and tensile stresses and in sensing the mechanical microenvironment.[12]

1.2.1 Cell-Topography Crosstalk

Cells perceive chemical and physical signals from neighboring cells, surrounding fluid and basement membranes, integrate these various stimuli and interpret them to generate appropriate cell responses.[13] Basement membranes consist of ECM components, including fibrous collagen, proteoglycans, laminin and fibronectin. In addition to biochemical and mechanical properties, basement membranes possess a complex, three-dimensional topography, because the membranes are a meshwork of pores, fibers, ridges and other features of micro-nanometer sized dimensions. Topographic features on synthetic surfaces influence cell behavior, in order to evaluate the effect of topography on cell fate in a distinct manner from that of the chemistry of the basement membrane.[14] The earliest surface morphology effect on cells was discovered almost a century ago when it was found that cells became oriented in response to the underlying topography.[15] This phenomenon is now commonly known as contact guidance.[16] The most extensively studied topographies are grooves and grids, protrusions and pit arrays. Three characteristic dimensions, namely ridge (or groove) width, inter-feature length (or pitch) and feature depth (or height), define linear topographies.[17] Different studies have documented that the topography of the substratum provides the cells with the ability to orient themselves, migrate and produce organized cytoskeletal arrangements.[14] In particular, it was shown that cell alignment is triggered by a combination of ridge width and groove depth and the threshold depth value for

whole cell alignment seems to be at a 35 nm.[13] Various cell types display contact guidance phenomenon when cultured on groove and ridge patterns with dimensions in the nanometer range. Profound differences in cytoskeletal organization have been found between cells elongated and aligned along these topographic features and cells cultured on smooth surfaces. Focal adhesions, actin microfilament bundles and microtubules have all been found to align along grooves and ridges, in cells aligned along these topographic features and the dimensions of the focal adhesions were determined by the width of the ridges. The percentage of aligned cells was constant on substrate topographies with lateral dimensions ranging from the nano- to the micro-scale and increased with groove depth. On flat substrates, cells and cytoskeleton did not display any preferred orientations.[18] The effect of other topographic models, such as pillars and pit, has also been analyzed in terms of cell proliferation. It increased with the decreasing diameter of the pit and cell attachment was greater on micro-scale pillars than on macro-scale pit.[13] Literature data clearly demonstrate the potency of topographic features in regulating the cell-material crosstalk and in directing and guiding cell fate. However, whether topography is an independent signal that is directly recognized by cell or it induces a pattern in the distribution of adhesive proteins present in cell culture medium is still unclear. In the first case cells should possess membrane sensors for topography recognition; on the other hand, it is know that the topographic patterns influence the distribution of serum adhesive protein, which, in turn, triggers pattern recognition via integrin recognition pathways.[17] Designing biomaterials with controlled topographic features, which reproduce physical and biochemical characteristics of the ECM, allow the elucidation of complex cell-material interaction mechanics by influencing several cell functions, such as migration, elongation and differentiation.

1.2.2 Cell Mechanical Properties

Mechanical properties, especially stiffness, of cells and their surrounding ECM contribute to the regulation of many important cell functions. Examples of biological functions regulated by external mechanic cues include cell proliferation, migration, spreading, morphology, differentiation and tissue homeostasis. Cell stiffness is largely dependent on the cytoskeleton, especially the networks of actin that consist of actin filaments directly underlying the cell membrane, attached via numerous membrane proteins.[19] Changes in cell stiffness are often signs associated with various disease conditions.[20] Several techniques have been used to study cell mechanics and underlying mechanisms, such as optical tweezers,[21] magnetic twisting cytometry,[22] micropipette aspiration[23] or optical stretcher technique.[24] Among all, atomic force microscopy (AFM) combines precise spatial resolution with high force sensitivity allowing the investigation of cell mechanical properties.[25] The basic principle is to indent a cell with an AFM tip of selected geometry and measure the applied force from the bending of the AFM cantilever. The AFM cantilever approaches the cell from a few nanometers above; makes contact with the cell; indents the cell so that the cantilever deflection reaches a preselected set point; and pulls away from the cell. During this process the cantilever deflection is recorded as a function of its location (Figure 1.1).

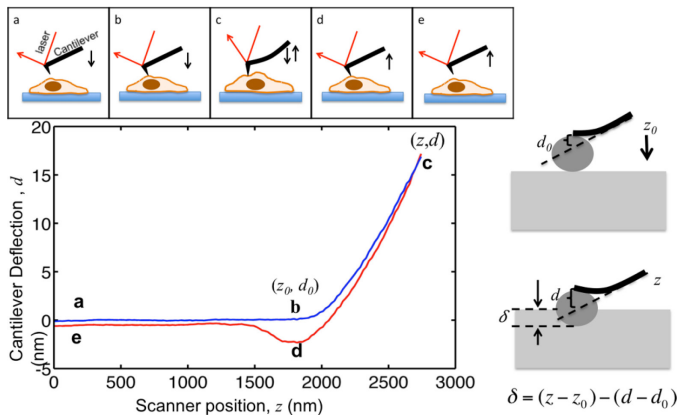

Figure 1.1 AFM Microindentation.[20]

The cantilevers are modeled as elastic beams so that their deflection is proportional to the force applied to the cell. The portion of the force-indentation curve from point b to point c in Figure 1.1, where the tip indents into the cell, is fit to the Hertz model for the corresponding tip geometry to give a quantitative measurements of stiffness.[20] The elastic modulus ($E_{elastic}$) is extracted from force (F) vs. indentation (δ) data using a modified Hertz model (Figure 1.2), where R is the relative radius of the tip and v is the Poisson's ratio, assumed to be 0.5 for an incompressible material. Parametric studies showed that varying v from 0.3 to 0.5 altered the measured properties by less than 20%.[26]

$$F(\delta) = \frac{4R^{1/2}E_{\text{elastic}}}{3(1-v^2)}\delta^{3/2}C$$

Figure 1.2 The force-indentation equation.[26]

This method has been widely applied to test the mechanical properties despite of its limitations such as uncertainty in contact point determination, applicability of the Hertz model and the possibility to physically damage the cells.[20]

It is known that topographic cues proved to be a powerful tool to control different aspects of the cell behavior, in particular micro and nano-topography can influence cell stiffness by modulating the focal adhesion formation and the structure of the cytoskeleton. For example, Rianna *et al.* reported that cells on micro-patterns were elongated, possessing a highly structured cytoskeleton and the elastic modulus values on cell body and nuclear regions were higher with respect to the cells on flat substrates.[27] Yim *et al.* explained that nanotopography induced changes in cytoskeletal organization and mechanical properties of human mesenchymal stem cells. In particular, changes in cytoskeletal organization were reflected in the cell mechanical properties, the stem cells exhibited lower elastic moduli when attached to nanopatterned surfaces as compared to unpatterned controls.[28] However, the

possible interplays between topography and cell stiffness have not been clarified yet.

1.3 Cell-Instructive Materials (CIMs)

Cell-Instructive Materials (CIMs) are biomaterials able to elicit a specific cell response, such as cell alignment and directed migration, or, ultimately, cell phenotype determination in order to understand the complex dynamic equilibrium between cells and the ECM.[17] Recent advancements in micro and nano-fabrication technologies allowed imprinting topographic features on cell-instructive materials to examine the role of topography in cell–material interactions.[29-30] Generally, these topographic features influence cell response in static manner, but recently, a new class of biomimetic materials, which are able to reproduce *in vitro* cell-material crosstalk due to the their potential to pattern surfaces in dynamic way, paves the way to fabrication of a next generation of CIMs.

1.3.1 "Static" Cell-Instructive Materials

In literature, the study of cell behavior on static topographic patterns has been widely analyzed, for example Curtis *et al.* published a review to explain the reaction of cells to their surrounding topography, in particular they considered a wide range of topographies but special attention was given to results on groove-ridge topographies.[31] Instead, Schulte *et al*. postulated that the initial cell adhesion on topographically patterned non adhesive hydrogel surfaces was mediated by protein adsorption and that this interaction could only persist due to the presence of surface topographic patterns.[32] Hamilton *et al*. investigated the adhesion, spreading and migration of human PDL fibroblasts in response to continuous and discontinuous topographical cues in the nanometric range. SEM and AFM images of the surfaces are shown in Figure 1.3.

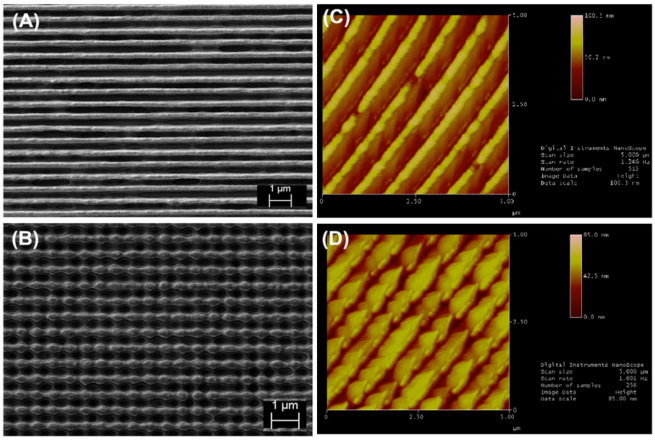

Figure 1.3 SEM and AFM images of the different topographies: (a-c) nanogrooves, and (b-d) discontinuous nanogrooves.[33]

Continuous nanogrooves had a depth of 100 nm, while discontinuous had features of 85 nm in depth. In both cases, the pitch was 50 nm.[33] On non-patterned substrates fibroblasts spread extensively characterized by large, mature FAs, with overall cell morphology showing no preferred direction.

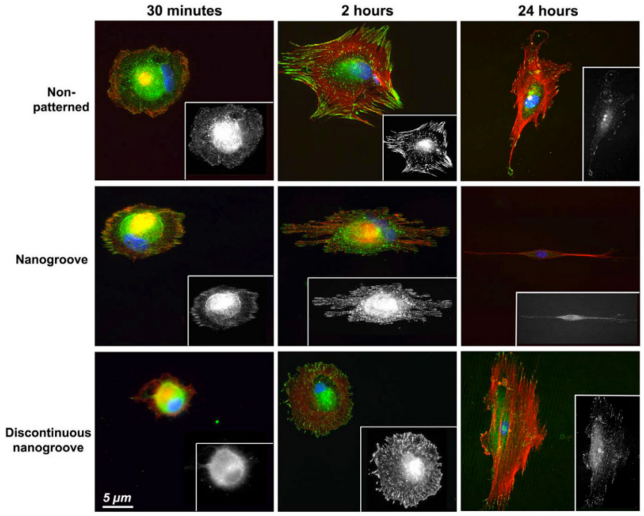

Figure 1.4 Influence of surface topography on PDL fibroblast attachment, spreading and FA formation.[33]

On nanogrooves highly aligned FAs were evident at the periphery of the cells, parallel to the groove long axis, but no obvious F-actin stress fibers were observed to have formed, while, on discontinuous nanogrooves, fibroblasts formed FAs, but overall morphology showed no preferred orientation (Figure 1.4). Teixeira *et al.*

also reported that cells responded to nanograting through alignment and elongation along the grating axis (Figure 1.5).[18]

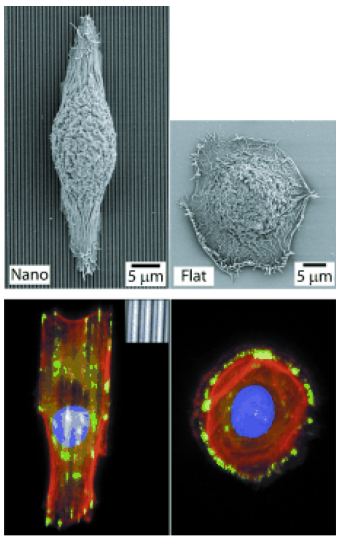

Figure 1.5 Cell−Nanograting response in epithelial cells. Adapted with permission form.[29] Angewandte Chemie International Edition.

Furthermore, Schulte *et al*. observed a remarkable unidirectional growth of murine fibroblasts along the oriented tubular channel into bulk hydrogels and an increase of their time survival, compared with cells embedded into non-structured gels.[34] Regarding cell morphology, it was verified that many cell types typically responded to nano-topography by simultaneously aligning and elongating in the groove direction. This response has been observed across numerous species and in various cell types, including preosteoblasts,[35] endothelial cells,[36] stem cells[37] and epithelial cells.[38]

The "static" cell instructive materials allow evaluating cell response but these *in vitro* studies are still far from recapitulating what actually occurs *in vivo*. The main disadvantage of "static" biomaterials is the inability to alter their properties in time and in the space, in fact, these properties cannot be readily modified *a posteriori* and the system reconfiguration cannot be controlled. For these reason "static" substrates do not allow mimicking the natural cell-extracellular interaction. In particular, no changes in topographical features can be observed once the cells are

seeded on them, therefore the cells cultivated on these patterned surfaces perceived the topographic features, in a static manner, and change their shape accordingly. On the other hand, in natural tissue, cells are exposed to signals, whose composition, strength, structure and localization change in time and space. The fabrication of biomaterials that can replicate this natural property would allow evaluating cell response and function in dynamic way.

1.3.2 "Dynamic" Cell-Instructive Materials

The human body represents a complex collection of dynamic environments where biochemical, physicochemical, and mechano-structural interactions serve to regulate cell behavior and fate,[39] in fact, the extracellular environment *in vivo* gradually changes its physicochemical properties in time. This dynamic nature, in turn, is closely related to tissue/organ development, regeneration, wound healing, and disease progression over time.[40] Therefore, dynamic platforms that have the potential to mimic the time-dependent variation of *in vivo* signaling may provide for an enhanced understanding of fundamental biological activities, such as cell adhesion, focal adhesions assembly, as well as cell migration and polarization[41] and could lead to eventual advances in tissue engineering and regenerative medicine. Recently, the scientific community has attempted to mimic cell-ECM crosstalk through the development of cell culture platforms with tunable properties. These material systems can change their properties on demand in response to user-defined triggers. Such triggers include: heat (temperature-responsive cell culture systems),[42-43] stress or pressure (mechano-responsive materials), electrical current/voltage (electro-responsive materials),[44] magnetic field (magneto-responsive materials), pH-change/solvent/moisture (chemo-responsive materials) and light (photo-responsive materials).[45] Importantly, these external stimuli are used as extremely mild, non-invasive triggers for cells and tissues in optimized conditions. Recent examples of dynamic cell culture platforms involve: tunable surface properties such as elasticity and topography, spatio-temporal presentation

and removal of biochemical signals, and applied force loading against cultured cells.[40] Therefore, stimuli-responsive materials or smart materials are powerful tools when designing the substrates of cell culture platforms. Particularly, topographic cues play an integral role in influencing cell fate. Current efforts, however, are centered on static patterns. The scientific community has recently shown an increased interest in developing surfaces with tunable topographies, because it is now possible to fabricate dynamic cell culture substrates with nanoscale topographies that can be readily modulated *in situ*, on cell-populated substrates directly, and study how cells respond to changes on surfaces upon which they interact. Lam *et al*. developed a reconfigurable, microtopographic system customized for cell culture that consisted of reversible wavy microfeatures on poly(dimethylsiloxane). The microfeatures were created by first oxidizing the PDMS substrate with plasma to form a brittle thin film before applying a compressive force on it. To return the substrate to a flat topography, the compression was simply removed. C_2C_{12} cells were able to align, unalign and realign themselves repeatedly while being cultured on the same substrate (Figure 1.6).[46]

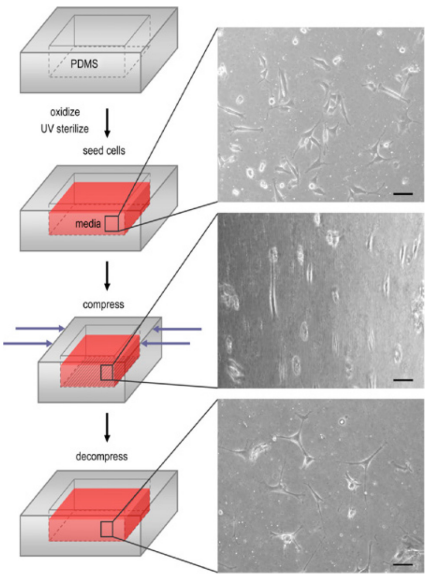

Figure 1.6 Schematic representation of the process of reversibly and cell response. Adapted with permission form.[46] Biomaterials.

While the topography could be controlled reversibly with this platform, pattern complexity and versatility was relatively simple and limited. Dynamic regulation of cell morphology can be achieved by utilizing substrates comprised of shape-memory polymers (SMPs), a class of "smart" materials, which have the unique ability to recover their original shape upon exposure to specific external stimuli. A great number of review reports the unique advantage on use of this supports to evaluate cell behavior, in particular, Davis *et al*. were one of the first to demonstrate this.[42]

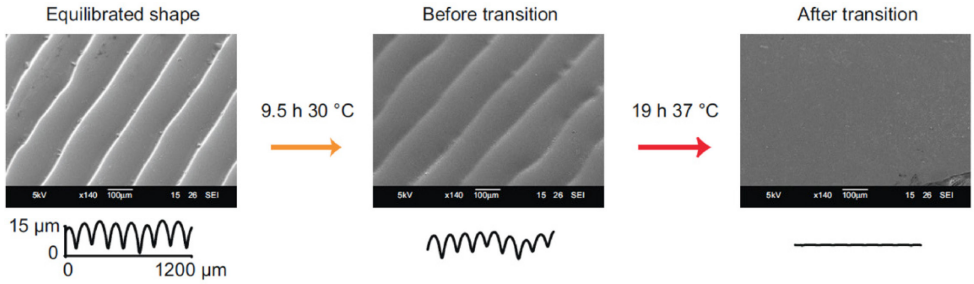

Figure 1.7 Cell culture substrate transitions from a grooved topography to a flat surface. Adapted with permission form.[42] Biomaterials.

After plating cells, the substrates triggered shape memory activation using a change in temperature tailored to be compatible with mammalian cell culture, by causing topographic transformation back to the original flat surface (Figure 1.7). This transition from a microgrooved to smooth topography significantly changed the alignment and cytoskeletal organization of mouse embryonic fibroblasts from a preferential alignment along the grooves to a more random, unaligned orientation, clearly demonstrating that SMP-based substrates potentially allow for a high degree of control over topographically-induced cellular behavior.[42] Le *et al.* developed thermally responsive PCL-SMP surfaces to dynamically probe cell-topography interactions. The substrate was then mechanically deformed at 130 ºC with a mold for the secondary, or temporary, shape before being cooled to -78 ºC. Afterwards, the substrate could be transition between the secondary and primary surface topographies by exposure to a 40 ºC environment. In this study, human

mesenchymal stem cells morphology switched from being highly aligned to stellate-shaped in direct response to a topographic transformation from an anisotropic groove array to a flat surface (Figure 1.8).[43]

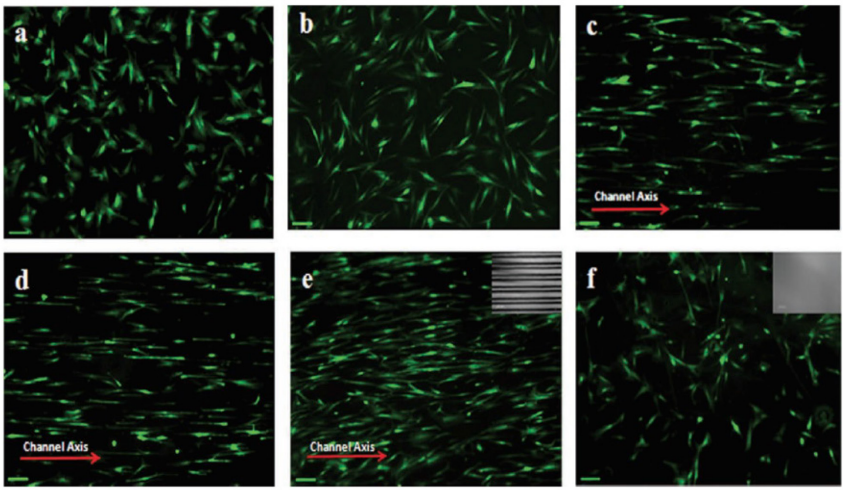

Figure 1.8 Fluorescent images of hMSCs. a) before, b) after heat treatment. Images of cells on static patterned surfaces c) before and d) after heat treatment. Cells on e) temporary channel SMP f) flat. Adapted with permission form.[43] Advanced Materials.

These PCL-SMP-based nanotopographic cues are capable of serving as instructive signals that dynamically regulate the structural and contractile properties of cells, in fact, Mengsteab *et al*. recently reported the neonatal rat ventricular myocytes (NRVMs) behavior into a well-defined anisotropic monolayer. Importantly, they found that the contractile direction of NRVM cell sheets was reorganized by the dynamic transition of their underlying topography. This result suggested that not only cardiac cellular function can be dynamically manipulated, but surface topography can influence tissue-level properties.[47] These shape-memory polymers relied on a dynamic modulation of surface topography, by switching between two reference configurations only. For these reasons, stimuli-responsive cell culture platforms with tunable topography are becoming one of the most powerful tools available for leading a new generation of dynamic systems capable of responding to external stimuli with temporal and spatial precision, because these systems have been shown to regulate not only cell alignment but also all cell functions. Among

several responsive materials, the attention has been focalized on the study of light responsive material, because light is one of the most promising stimuli to produce dynamic platforms, so it can be precisely localized over a substrate, programmed in time, remotely addressable and it is not harmful for cells at a proper wavelength.

1.4 Azopolymers

Light-responsive materials are usually classified by the molecules they employ in achieving their photo-responsive properties. One of the most widely light response materials used are azopolymers, they are polymers that have an azobenzene groups within the polymer structure.

1.4.1 Azobenzene

Azobenzene is an aromatic molecule formed by an azo linkage (N-N) connecting two phenyl rings. Azobenzene has two isomeric states: a metastable cis form and a thermally stable trans configuration (Figure 1.9). The azobenzenes can interconvert between these isomers upon absorption of a photon. The molecule undergoes trans-cis isomerization when irradiated with light tuned to an appropriate wavelength. The reverse cis-trans isomerization can be driven by light or it occurs spontaneously in the dark owing to the thermodynamic stability of the trans isomer.[48]

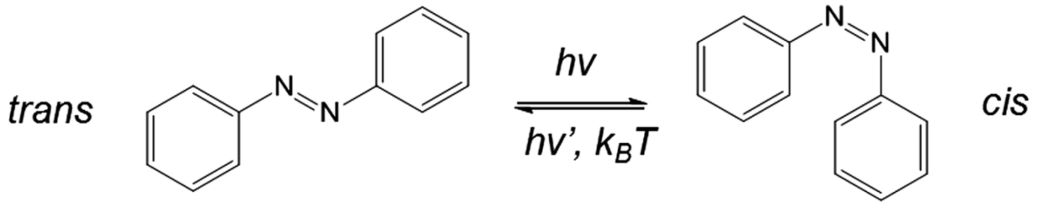

Figure 1.9 Structure of azobenzenes. Adapted with permission form.[48] Chemical Society Reviews.

The trans isomer is more stable by approximately 50-100 kJ/mol[49] and the energy barrier to the photo-excited state (barrier to isomerization) is of the order of

200 kJ/mol. Thus, in the dark, most azobenzene molecules will be found in the trans form.[50] Azobenzenes can be separated into three spectroscopic classes characterized by the thermal relaxation of the cis to the trans isomer and the wavelength of absorption triggering the trans to cis isomerization:

- Azobenzene-type molecules absorb in the UV range and their cis form can be stable for days in the dark.
- Amino-azobenzenes have an intermediate lifetime and a slight red shift in the trans absorption band.
- Pseudo-stilbenes have a very fast thermal reconversion and a far-red shifted absorption.

Many azobenzenes exhibit absorption characteristics similar to those of the unsubstituted azobenzene archetype.[51] These trans-cis photoisomerizations usually have picosecond timescales.[52] Alternatively, azobenzene molecules will thermally reconvert from the cis to the trans state, with a timescale ranging from milliseconds to hours, depending on the substitution pattern and local environment. More specifically, the lifetimes for azobenzenes, aminoazobenzenes and pseudo-stilbenes are usually on the order of hours, minutes and seconds, respectively.[53]

1.4.1.1 Photo Orientation of Azobenzene Molecules

Azobenzene chromophores can be oriented using a coherent light (Figure 1.10). Azobenzenes preferentially absorb light polarized along their transition dipole axis (long axis of the azo-molecule). The probability of absorption varies as $\cos^2\alpha$, where α is the angle between the light polarization and the azo dipole axis. Thus, azo-molecules orientated along the polarization of the light will absorb, convert into the cis form and after they revert to the trans form with a new random direction. The azo-molecules orientated perpendicularly to the light polarization will not absorb. The chromophores with dipole axis perpendicular to the light polarization direction will no longer be isomerized and reorient. Thus, there is a net

depletion of chromophores aligned with the light polarization, with a concomitant increase in the population of chromophores aligned perpendicular.[52]

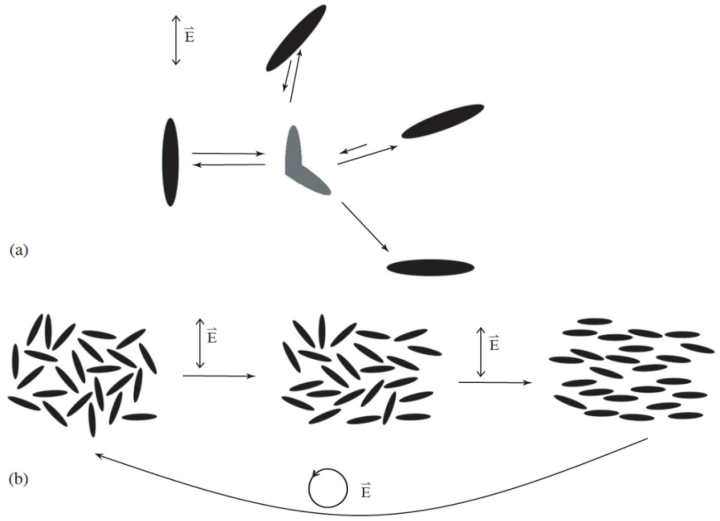

Figure 1.10 Statistical photo-orientation of azobenzene molecules. (a) The molecules aligned along the polarization direction of the incident light absorb. (b) Irradiation of an isotropic.[53]

The orientation due to polarized light is reversible; in fact, using a different polarization direction it is possible to modify the direction of azo-molecules axis. Circularly polarized light and incoherent and unpolarized light randomize the chromophore orientations.[54]

1.5 Photoinduced Deformation In Azopolymers Films

The azobenzene photoisomerization can have a wide range of unexpected possible consequences.[55] The literature reports different views on the mechanism of light induced polymer deformation. Hurduc's group supports that the isomerization of azobenzenes causes an athermal transition of the glassy azobenzenes-containing polymer into a fluid state.[56] Santer's group supports the re-orientational model, where the surfaces mass transport of the polymer accomplished during polymer deformation is generated by the light-induced re-orientation of the azobenzene side

chains.[57] Galinski *et al.* explained the photoactivated pattern formation on azopolymer films by the microphase separation of the coexisting trans and cis isomers in the surface layer of the film.[58] Several theories have been developed to unravel the mechanism of photoinduced mass-migration of azobenzene containing polymer chains and pattern inscription, nevertheless, a complete elucidation of the phenomenon of pattern formation that takes into consideration all the involved aspects is still lacking.

1.5.1 Surface Mass Transport

The azofilms exhibit a unique and remarkable surface-mass transport on a micrometer and submicrometer length scale under a proper light illumination. The surface mass transport involves repeated trans-cis photoisomerization of azobenzene.[59] This is a reversible phenomenon[53], in fact, the topographic features embossed can be erased by heating the sample above glass transition temperature (Tg). A circular polarized light or an incoherent light source can also revert the topography surface to its initial flat profile by a randomization of the azobenzenes. After the erasing, the azofilms show no evidence of degradation or charring of the polymer films.[60]

1.5.1.1 Interference Lithography

In 1995, surface mass transport was discovered in polymer thin films containing the azobenzenes when the substrates were irradiated with a light interference pattern.[60-61] Two coherent laser beams, with a wavelength in the azo-absorption band, were intersected at the sample surface. The sinusoidal light interference pattern at the sample surface led to a sinusoidal surface patterning, a surface relief grating (SRG). The process occurred readily at room temperature with moderate irradiation (1-100 mW/cm^2) over seconds to minutes.[57] When photosensitive azobenzene-containing polymers are irradiated with light interference patterns, topographic variations of film follow the distribution of intensity or polarization of

the interference pattern, because the light is able to orient the azobenzenes in a different way (re-orientational theory) and confines the material motion in a specific direction (anisotropic photofluidization theory). Under continuous irradiation, the multiple photoisomerization transitions are accompanied by changes in size and in polarity of the azobenzene molecules and result in a locally preferred orientation of the azo-groups with their main axis perpendicular to the E-field vector.[62] The structuring of topography due to mass transport phenomenon occurs in a regular and periodic fashion across the polymer surface over the full area of illumination, specifically in an interference pattern there are alternating bright and dark areas and recent experimental data confirmed that the material tends to accumulate in the dark regions, probably in order to relax the stress, which accumulates from the isomerization movements.[57] The position of minimal intensity of the interference patterns corresponds to highest topography, whereas the positions of maximal intensity can be related to negligible topography.[62]

1.5.1.2 Focused Laser Beam

A single Gaussian laser beam can induce an azosurface deformation, by aligning the azobenzene groups in the direction perpendicular to the polarization of the incident light.[59] This technique presents different unique advantages in comparison to the other photopatterning technique.

- The Gaussian beam has a symmetric intensity distribution, which allows to have a definite reference position.[63]
- The intensity distribution and size of a Gaussian laser beam can be explicitly calculated according to the laser propagation theory.[64]
- Its non contact feature allows a true free surface of the polymer to be manipulated and avoids any probable restraint and defects caused by other contact methods, e.g., using a transmission mask.[64]

- The single laser beam setup is very simple and removes any issues connected to the mechanical instabilities of the optical elements.[65]

It is known that the mass migration process depends on the light polarization, intensity and wavelength. The photoinduced surface deformation occurs in the direction of the light polarization; in fact, the exposure with a polarization perpendicular to the direction of the light intensity does not produce appreciable surface variation. Brian *et al*. verified that the surface modification depends from the laser beam polarization and intensity, by illuminating the polymer surface by a focused light spot. Focused beam was able to make a hole in correspondence to the center of the laser spot and the surface deformation was influenced by the polarization of the laser beam (Figure 1.11). The spot carried out had two lobes that piled up away from high intensity area along the polarization direction and these lobes did not appear when using a circular polarized Gaussian beam.[63]

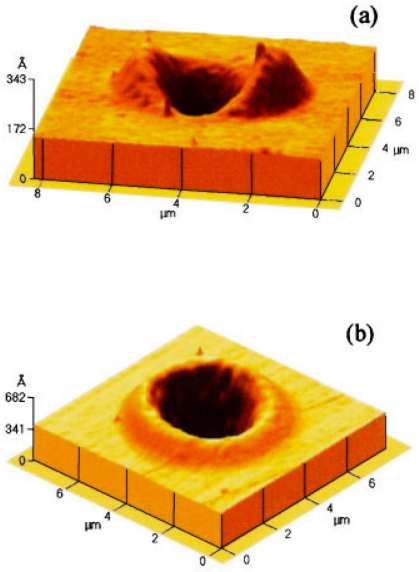

Figure 1.11. Surface deformation induced by Gaussian beams with low intensity. (a) Linear polarization; (b) circular polarization. Adapted with permission form.[63] Applied Physics Letters.

Instead, the polymer surface deformation induced by a higher intensity polarized Gaussian laser presented a central peak in the surface profile and the polymer in the center of the exposed spot became optically bleached (Figure 1.12).[64]

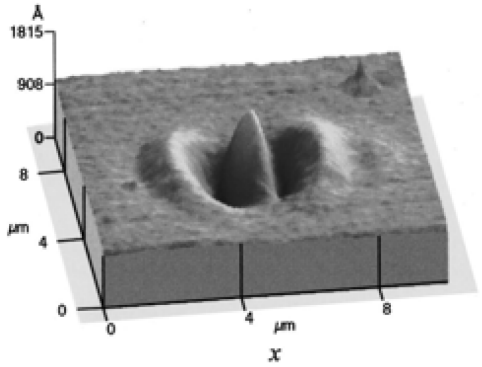

Figure 1.12 Surface deformation induced by linearly polarized Gaussian beam with high intensity. Adapted with permission form.[64] Journal of Applied Physics.

The mechanism to explain the appearance of peaks at the center of regions are not clear, however, this phenomenon may be due to the high-intensity photothermal effects and photochemical reaction such as degradation and bleaching of the chromophores. Photocrosslinking or photothermally induced crosslinking may also occur. These are plausible because the large quantity of energy absorbed from high laser irradiance would result in an increase of the temperature of the material during the exposure.[64] The focused laser beam allows embossing linear pattern by moving the sample with respect to the light polarization direction and the lateral size of the induced surface deformation is approximately equal to the diameter of the Gaussian beam (Figure 1.13).[63]

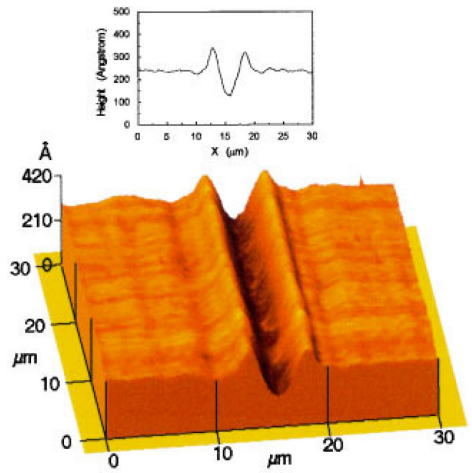

Figure 1.13 Surface deformation induced by a one-dimensional Gaussian beam. Adapted with permission form.[63] Applied Physics Letters.

Recently, Noga *et al*. demonstrated that the characteristics of the topographic topographies can be changed by adjusting the value of one or more of the following parameters: the thickness of the polymer layer, the temperature and the wavelength of laser beam.[65] This optical technique produced topographic features of different shape on the surface by controlling the position of the sample respect to the focalized laser beam. Specifically, the following image (Figure 1.14) shows the topography and the cross-section profile of five adjacent lines, each line is a trench, about 480 nm wide, obtained moving the sample perpendicularly to the polarization direction. These trenches were characterized by the accumulation of material at the edges of trench. The mass migration phenomenon was clearly appreciable by analyzing the surface profile above and below the red dotted line (Figure 1.14). The value at red line (80 nm) represents the level of the unaltered polymer surface.[66]

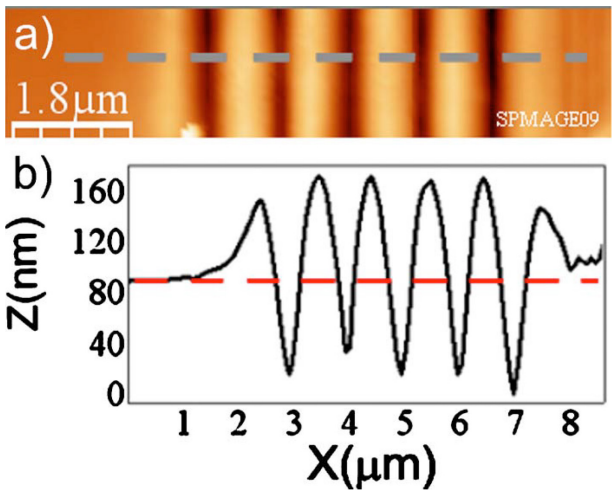

Figure 1.14 (a) AFM image of trenches (b) profile along the gray dotted line in (a). Adapted with permission form.[66] Journal of Applied Physics.

Instead, a different material response was obtained moving the sample along the polarization direction of laser. For this configuration of the scanning direction with respect to the laser polarization, the features were bumps whose lateral size is comparable to the linear dimensions of the diffraction-limited focused laser spot, about 200 nm (Figure 1.15).[66]

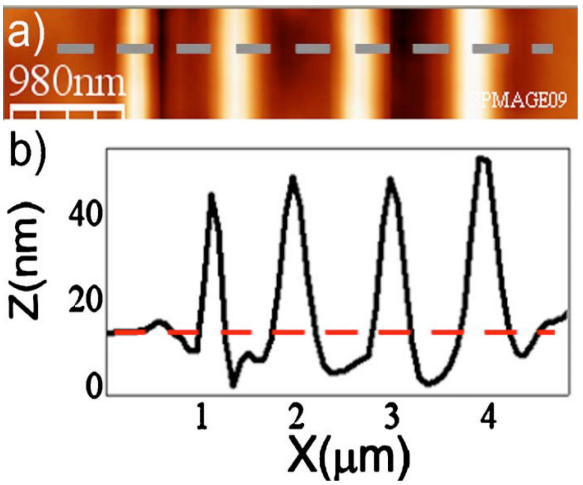

Figure 1.15. (a) AFM image of trenches (b) profile along the gray dotted line in (a). Adapted with permission form.[66] Journal of Applied Physics.

After the first stage of modification, the samples can be turned by 90° with respect to previous orientation and new laser scanning can performed perpendicularly to previous by obtaining a different topographical feature.[67]

In our experiments, instead, the focused beam of a confocal microscope was directly used in order to write complex topographic patterns on the azosurface. The mass transport induced by the azobenzene isomerization was activated only inside drawn regions-of-interest (ROIs) in which the focused laser beam was scanned by means of galvanometric mirrors. This optical set-up let us to control position of the laser beam in order to emboss on the sample topographic features of various shape.

1.6 Azopolymers as Cell-Instructive Materials (CIMs)

Azopolymers have been used in many biological applications such as the fabrication of photosensitive micelles skilled to encapsulate and provide controlled release of small molecules pointing to their potential use in drug delivery applications,[68] or even for photocontrol of biomolecular structures (e.g. switching between two peptide configurations).[68-69] However, works in which azopolymers are used, as cell-instructive materials, even though really promising, are still very

few. Barillé *et al.* presented an easy technique to produce erasable and directly *in vitro* submicron-scale surface relief gratings for the guidance of neurons. The photo-chemical conversion of the azo-chromophores induces a large-scale mechanical response of substrates and leads to a large-scale mass transport of thin azofilms when exposed to light.[70] The substrates were biocompatible and on the nanoscale groove sample cells began to differentiate with extended neuritis, which were developed along the network (Figure 1.16).

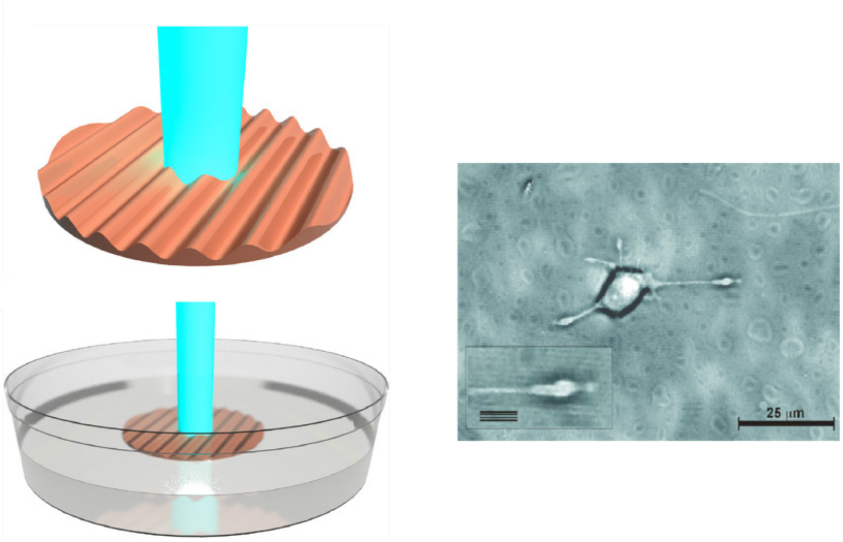

Figure 1.16 Scheme of the set-up to create a surface relief grating with a single laser beam and cell behavior on nanoscale grooves. Adapted with permission form.[70] Colloids and Surfaces B: Biointerfaces.

Another example of the use of azomaterials as cell culture supports for future dynamic applications came from Baac *et al.* where the laser holography on a photo-responsive azobenzene copolymeric layer has been employed to produce surface relief grating (SRG), which had a regular sinusoidal shape, to evaluate cell orientation. The primary human astrocytes were densely populated with random orientation forming multiple layers over the whole flat substrate, while on the SRG regions the cell proliferation was still toward the groove direction (Figure 1.17).[71]

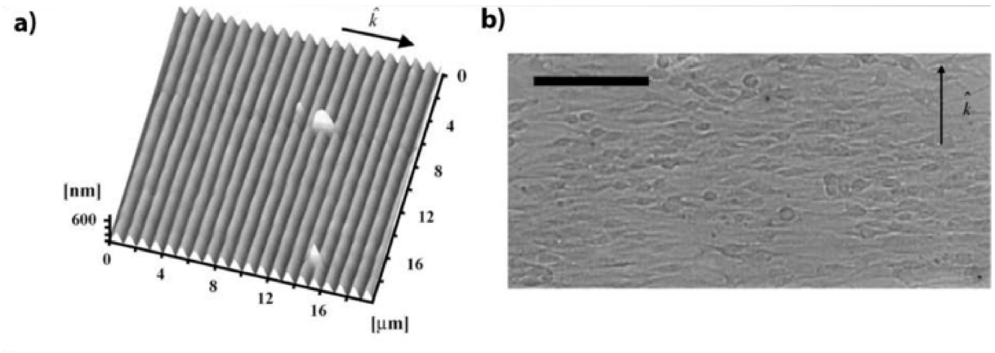

Figure 1.17. (a) AFM image of SRG region (b) Cell behavior on SRG. Adapted with permission form.[71] Materials Science and Engineering: C.

Rocha *et al.* demonstrated the potential of azo-supports for biological application, because the polymers can provide optically active supports to facilitate the understanding of the complex mechanisms involved in the interaction between cells and their environment. Images shown in Figure 1.18 evidences the influence of the azopolymer substrates with different structures on hepatic cells behavior.[68]

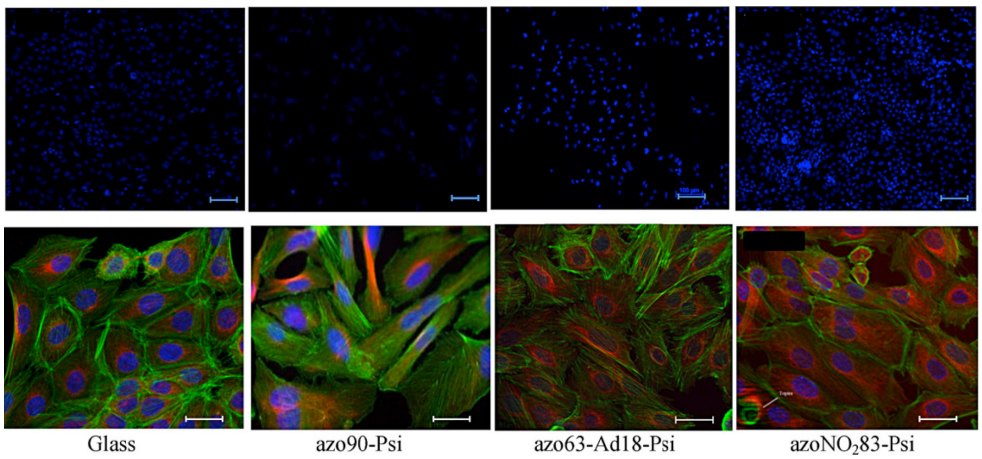

Figure 1.18 Immunofluorescense microscopy images of cells grown on a control and on azofilms with different structures. Adapted with permission form.[68] Journal of Photochemistry and Photobiology A: Chemistry.

Furthermore, preliminary studies on the use of novel stimuli-responsive biomaterials, azobenzene-containing polymer brushes, have performed. SRG patterns could be inscribed on these synthesized azopolymer brushes and mechanically erased by ultrasonication.[72] A work recently published by our group, showed the use of SRG on pDR1m azopolymer for cell culture application.[73]

Topographic patterns were inscribed on films by using an interference pattern of light, Lloyd's mirror. To use these materials as cell culture substrates, preliminary tests to assess pattern stability under conditions comparable to those experienced during cell culture, were performed. Different topographic patterns were embossed on azopolymer films to exert a strong influence on fibroblast behavior.

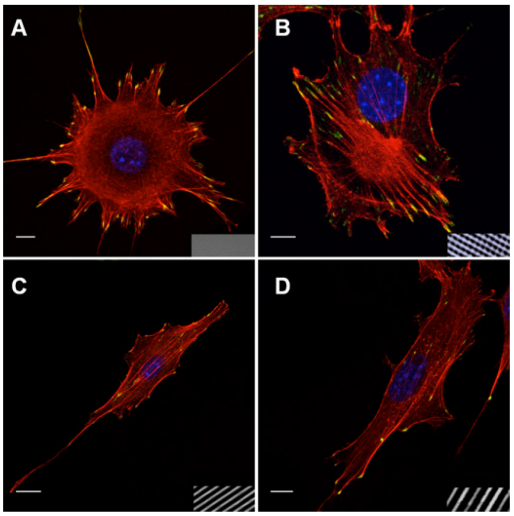

Figure 1.19 Confocal images of NIH-3T3 on (A) flat pDR1m, (B) grid pattern, and (C) 2.5 μm and (D) 5.5 μm linear patterns. Adapted with permission form.[73] American Chemical Society.

Cells were mostly round or elliptical in shape when cultivated on flat or grid pattern (Figure 1.19 A-B), whereas they appeared to be polarized and elongated along the direction of linear patterns (Figure 1.19 C-D). Circularly polarized light was used to induce pattern erasure on pDR1 films. The quantification of cell elongation and orientation was shown, in which the highest values of elongation were measured on the linear pattern, whereas the elongation of cells on the erased pattern was not significantly different from that of the flat case (Figure 1.20). Accordingly, cell orientation was nearly parallel to the pattern direction with a narrow distribution when cells were seeded on the pattern, while a random orientation with a broad distribution was measured for cells on both flat and erased pattern. FA length did not display changes in the writing/erasing cycles, whereas FA orientation was very sensitive to the topography as parallel FAs were observed

on the SRG only (Figure 1.20). In principle, the photoswitching has a great potential that needs to be implemented for dynamic changes of the pattern features.

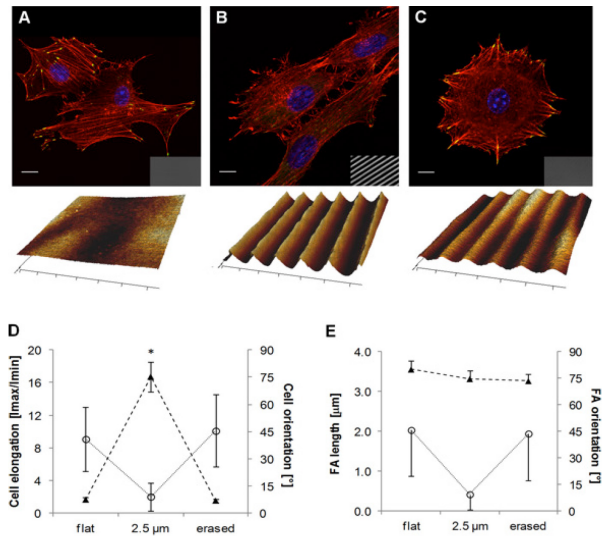

Figure 1.20 Confocal images of NIH-3T3 on (A) flat, (B) SRG gratings, and (C) pattern erased with circularly polarized light. (D) Plots of cell elongation (▲) and cell orientation (○). (E) Plot of FA length (▲) and orientation (○). Adapted with permission form.[73] American Chemical Society.

The first example of systems that presented a versatile way to change surface topography both in a reversible and irreversible fashion were azobenzene based liquid crystal polymer network (LCN). The adaptive and programmable nature of these light responsive LCN coatings was employed to achieve new spatially arranged patterned biointerfaces for *in situ* temporal control of surface properties in order to guide cell behavior. Cell adhesion and migration were studied either on surfaces with predefined (fixed) microscale topographic cues or on surfaces where at a specific point in time the surface structure was changed *in situ*. Preliminary experiments on patterned LCN surfaces showed that it was also possible to form photoswitchable (reversible) topographies on demand at the nanoscale.[74] Finally, pDR1 films can be used as dynamic support to study live cells in real-time and investigate the complex aspects of the spatio-temporal variations actuated *in vivo*.[75] This approach based on a novel photopatterning methodology that exploit the focused laser beam of the confocal microscope set-up will be described in detail in the next chapters of this thesis.

1.7 Aim and Outline of the Thesis

The aim of my work is to fabricate and characterize different topographic patterns on dynamic light-switchable support using a confocal microscope optical set-up. One of the major challenges nowadays is the *in vitro* reproduction of the dynamic interplay between cells and extracellular environment. In particular, the literature reports that the topographic signals plays an important role in affecting cell functions and fate.[29] Dynamic biomaterials are indeed required for a control of cell behavior *in vitro*, simulating the complexity of natural ECM remodeling.[2] In this respect, azobenzene-based biointerfaces are attracting attention, because they are capable of many changes in their topographic properties upon the application of light. In particular, the versatility of laser-based confocal microscope technique allows inducing spatio-temporal dynamic topographic changes *in situ*, both in time and space, during cell culture. In this thesis, different patterns can be designed on cell-populated azopolymer films with high control on time, space and on-off signal modification in order to evaluate the cell response to these dynamic topographic cues, which can be remodeled on demand. Following, the outline of the thesis is reported with a brief description of each chapter. The **Chapter 1** of this thesis presents an introduction on azobenzene-containing materials with an overview of the photoinduced deformation in azo-materials surfaces. Then, the recent use of these photoresponsive materials as cell culture substrates is presented and their potential applications are highlighted. In **Chapter 2** azopolymer films are used as cell culture supports. Initially, the cell response to static pattern is evaluated and the biocompatibility of these systems is confirmed. Finally, the potential application of these materials as dynamic platform is reported, by guiding cell behavior in real-time. In **Chapter 3** several circular patterns are produced in order to evaluate the most appropriate pattern size perceived by cells and different cell functions, such as area, elongation and alignment, to this modular topographies are analyzed in time. Recent discoveries confirm that curvature can influence cell behavior not only in

terms of adhesion and migration but also in terms of differentiation and expression of carcinogenicity. In **Chapter 4**, instead, topographic patterns on azopolymers films prove to influence cell mechanical properties, besides adhesion and orientation. A study on cytoskeleton assembly is reported in order to correlate cell elastic properties with cell shape and organization. Furthermore, changes of focal adhesion orientation are evaluated, during the first hour from pattern inscription. In **Conclusion and Future Perspectives** a summary of the main results achieved in this thesis are presented and future applications are proposed.

1.8 References

1. Peppas, N. A.; Langer, R., New challenges in biomaterials. *Science-AAAS-Weekly Paper Edition-including Guide to Scientific Information* **1994,** *263* (5154), 1715-1719.

2. Lutolf, M.; Hubbell, J., Synthetic biomaterials as instructive extracellular microenvironments for morphogenesis in tissue engineering. *Nature Biotechnology* **2005,** *23* (1), 47.

3. Vacanti, J. P.; Langer, R., Tissue engineering: the design and fabrication of living replacement devices for surgical reconstruction and transplantation. *The Lancet* **1999,** *354*, S32-S34.

4. Andrade, J.; Hlady, V., Protein adsorption and materials biocompatibility: a tutorial review and suggested hypotheses. In *Biopolymers/Non-Exclusion HPLC*, Springer: 1986; pp 1-63.

5. Burdick, J. A.; Murphy, W. L., Moving from static to dynamic complexity in hydrogel design. *Nature Communications* **2012,** *3*, 1269.

6. Langer, R.; Tirrell, D. A., Designing materials for biology and medicine. *Nature* **2004,** *428* (6982), 487.

7. Kleinman, H. K.; Philp, D.; Hoffman, M. P., Role of the extracellular matrix in morphogenesis. *Current Opinion in Biotechnology* **2003,** *14* (5), 526-532.

8. Ventre, M.; Netti, P. A., Engineering cell instructive materials to control cell fate and functions through material cues and surface patterning. *ACS Applied Materials & Interfaces* **2016,** *8* (24), 14896-14908.

9. Geiger, B.; Yamada, K. M., Molecular architecture and function of matrix adhesions. *Cold Spring Harb Perspect Biol* **2011,** *3* (5).

10. Sackmann, E.; Bruinsma, R. F., Cell adhesion as wetting transition? *Chemphyschem* **2002,** *3* (3), 262-9.

11. Wheeldon, I.; Farhadi, A.; Bick, A. G.; Jabbari, E.; Khademhosseini, A., Nanoscale tissue engineering: spatial control over cell-materials interactions. *Nanotechnology* **2011,** *22* (21), 212001.

12. Fletcher, D. A.; Mullins, R. D., Cell mechanics and the cytoskeleton. *Nature* **2010,** *463* (7280), 485-92.

13. Loesberg, W. A.; te Riet, J.; van Delft, F. C.; Schon, P.; Figdor, C. G.; Speller, S.; van Loon, J. J.; Walboomers, X. F.; Jansen, J. A., The threshold at which substrate nanogroove dimensions may influence fibroblast alignment and adhesion. *Biomaterials* **2007,** *28* (27), 3944-51.

14. Flemming, R. G.; Murphy, C. J.; Abrams, G. A.; Goodman, S. L.; Nealey, P. F., Effects of synthetic micro- and nano-structured surfaces on cell behavior. *Biomaterials* **1999,** *20* (6), 573-88.

15. Singhvi, R.; Stephanopoulos, G.; Wang, D. I., Effects of substratum morphology on cell physiology. *Biotechnology and Bioengineering* **1994,** *43* (8), 764-771.

16. Weiss, P., Cell contact. *International Review of Cytology* **1958,** *7*, 391-423.

17. Ventre, M.; Causa, F.; Netti, P. A., Determinants of cell-material crosstalk at the interface: towards engineering of cell instructive materials. *J R Soc Interface* **2012,** *9* (74), 2017-32.

18. Teixeira, A. I.; Abrams, G. A.; Bertics, P. J.; Murphy, C. J.; Nealey, P. F., Epithelial contact guidance on well-defined micro- and nanostructured substrates. *J Cell Sci* **2003,** *116* (Pt 10), 1881-92.

19. Lekka, M.; Laidler, P.; Gil, D.; Lekki, J.; Stachura, Z.; Hrynkiewicz, A., Elasticity of normal and cancerous human bladder cells studied by scanning force microscopy. *European Biophysics Journal* **1999,** *28* (4), 312-316.

20. Thomas, G.; Burnham, N. A.; Camesano, T. A.; Wen, Q., Measuring the mechanical properties of living cells using atomic force microscopy. *Journal of Visualized Experiments: JoVE* **2013,** (76).

21. Zhang, H.; Liu, K.-K., Optical tweezers for single cells. *Journal of The Royal Society Interface* **2008,** *5* (24), 671-690.

22. Laurent, V. r. M.; Hénon, S.; Planus, E.; Fodil, R.; Balland, M.; Isabey, D.; Gallet, F. o., Assessment of mechanical properties of adherent living cells by bead micromanipulation: comparison of magnetic twisting cytometry vs optical tweezers. *Journal of Biomechanical Engineering* **2002,** *124* (4), 408-421.

23. Hochmuth, R. M., Micropipette aspiration of living cells. *Journal of Biomechanics* **2000,** *33* (1), 15-22.

24. Guck, J.; Ananthakrishnan, R.; Mahmood, H.; Moon, T. J.; Cunningham, C. C.; Käs, J., The optical stretcher: a novel laser tool to micromanipulate cells. *Biophysical Journal* **2001,** *81* (2), 767-784.

25. Schillers, H.; Rianna, C.; Schäpe, J.; Luque, T.; Doschke, H.; Wälte, M.; Uriarte, J. J.; Campillo, N.; Michanetzis, G. P.; Bobrowska, J., Standardized Nanomechanical Atomic Force Microscopy Procedure (SNAP) for Measuring Soft and Biological Samples. *Scientific Reports* **2017,** *7*.

26. González-Cruz, R. D.; Fonseca, V. C.; Darling, E. M., Cellular mechanical properties reflect the differentiation potential of adipose-derived mesenchymal stem cells. *Proceedings of the National Academy of Sciences* **2012,** *109* (24), E1523-E1529.

27. Rianna, C.; Ventre, M.; Cavalli, S.; Radmacher, M.; Netti, P. A., Micropatterned azopolymer surfaces modulate cell mechanics and cytoskeleton structure. *ACS Applied Materials & Interfaces* **2015,** *7* (38), 21503-21510.

28. Yim, E. K.; Darling, E. M.; Kulangara, K.; Guilak, F.; Leong, K. W., Nanotopography-induced changes in focal adhesions, cytoskeletal organization, and mechanical properties of human mesenchymal stem cells. *Biomaterials* **2010,** *31* (6), 1299-1306.

29. Bettinger, C. J.; Langer, R.; Borenstein, J. T., Engineering substrate topography at the micro-and nanoscale to control cell function. *Angewandte Chemie International Edition* **2009,** *48* (30), 5406-5415.

30. Yao, X.; Peng, R.; Ding, J., Cell–material interactions revealed via material techniques of surface patterning. *Advanced Materials* **2013,** *25* (37), 5257-5286.

31. Curtis, A.; Wilkinson, C., Topographical control of cells. *Biomaterials* **1997,** *18* (24), 1573-1583.

32. Schulte, V. A.; Diez, M.; Möller, M.; Lensen, M. C., Topography-Induced Cell Adhesion to Acr-sP (EO-stat-PO) Hydrogels: The Role of Protein Adsorption. *Macromolecular Bioscience* **2011,** *11* (10), 1378-1386.

33. Hamilton, D. W.; Oates, C. J.; Hasanzadeh, A.; Mittler, S., Migration of periodontal ligament fibroblasts on nanometric topographical patterns: influence of filopodia and focal adhesions on contact guidance. *PLoS One* **2010,** *5* (12), e15129.

34. Schulte, V. A.; Alves, D. F.; Dalton, P. P.; Moeller, M.; Lensen, M. C.; Mela, P., Microengineered PEG hydrogels: 3D scaffolds for guided cell growth. *Macromolecular Bioscience* **2013,** *13* (5), 562-572.

35. Ventre, M.; Natale, C. F.; Rianna, C.; Netti, P. A., Topographic cell instructive patterns to control cell adhesion, polarization and migration. *Journal of the Royal Society Interface* **2014,** *11* (100), 20140687.

36. Biela, S. A.; Su, Y.; Spatz, J. P.; Kemkemer, R., Different sensitivity of human endothelial cells, smooth muscle cells and fibroblasts to topography in the nano–micro range. *Acta Biomaterialia* **2009,** *5* (7), 2460-2466.

37. Iannone, M.; Ventre, M.; Formisano, L.; Casalino, L.; Patriarca, E. J.; Netti, P. A., Nanoengineered surfaces for focal adhesion guidance trigger mesenchymal stem cell self-organization and tenogenesis. *Nano Letters* **2015,** *15* (3), 1517-1525.

38. Clark, P.; Connolly, P.; Curtis, A.; Dow, J.; Wilkinson, C., Cell guidance by ultrafine topography in vitro. *Journal of Cell Science* **1991,** *99* (1), 73-77.

39. Gattazzo, F.; Urciuolo, A.; Bonaldo, P., Extracellular matrix: a dynamic microenvironment for stem cell niche. *Biochimica et Biophysica Acta (BBA)-General Subjects* **2014,** *1840* (8), 2506-2519.

40. Uto, K.; Tsui, J. H.; DeForest, C. A.; Kim, D.-H., Dynamically tunable cell culture platforms for tissue engineering and mechanobiology. *Progress in Polymer Science* **2017,** *65*, 53-82.

41. Gooding, J. J.; Parker, S. G.; Lu, Y.; Gaus, K., Molecularly engineered surfaces for cell biology: From static to dynamic surfaces. *Langmuir* **2013,** *30* (12), 3290-3302.

42. Davis, K. A.; Burke, K. A.; Mather, P. T.; Henderson, J. H., Dynamic cell behavior on shape memory polymer substrates. *Biomaterials* **2011,** *32* (9), 2285-2293.

43. Le, D. M.; Kulangara, K.; Adler, A. F.; Leong, K. W.; Ashby, V. S., Dynamic Topographical Control of Mesenchymal Stem Cells by Culture on Responsive Poly (ϵ-caprolactone) Surfaces. *Advanced Materials* **2011,** *23* (29), 3278-3283.

44. Ng, C. C. A.; Magenau, A.; Ngalim, S. H.; Ciampi, S.; Chockalingham, M.; Harper, J. B.; Gaus, K.; Gooding, J. J., Using an electrical potential to reversibly switch surfaces between two states for dynamically controlling cell adhesion. *Angewandte Chemie International Edition* **2012,** *51* (31), 7706-7710.

45. Vaselli, E.; Fedele, C.; Cavalli, S.; Netti, P. A., "On–Off" RGD Signaling Using Azobenzene Photoswitch-Modified Surfaces. *ChemPlusChem* **2015,** *80* (10), 1547-1555.

46. Lam, M. T.; Clem, W. C.; Takayama, S., Reversible on-demand cell alignment using reconfigurable microtopography. *Biomaterials* **2008,** *29* (11), 1705-1712.

47. Mengsteab, P. Y.; Uto, K.; Smith, A. S.; Frankel, S.; Fisher, E.; Nawas, Z.; Macadangdang, J.; Ebara, M.; Kim, D.-H., Spatiotemporal control of cardiac anisotropy using dynamic nanotopographic cues. *Biomaterials* **2016,** *86*, 1-10.

48. Bandara, H. D.; Burdette, S. C., Photoisomerization in different classes of azobenzene. *Chemical Society Reviews* **2012,** *41* (5), 1809-1825.

49. Mahimwalla, Z.; Yager, K. G.; Mamiya, J.-i.; Shishido, A.; Priimagi, A.; Barrett, C. J., Azobenzene photomechanics: prospects and potential applications. *Polymer Bulletin* **2012**, 1-40.

50. Xie, S.; Natansohn, A.; Rochon, P., Recent developments in aromatic azo polymers research. *Chemistry of Materials* **1993,** *5* (4), 403-411.

51. Goulet-Hanssens, A.; Barrett, C. J., Photo-control of biological systems with azobenzene polymers. *Journal of Polymer Science Part A: Polymer Chemistry* **2013,** *51* (14), 3058-3070.

52. Kobayashi, T.; Degenkolb, E.; Rentzepis, P., Picosecond spectroscopy of 1-phenylazo-2-hydroxynaphthalene. *Journal of Physical Chemistry* **1979,** *83* (19), 2431-2434.

53. Yager, K. G.; Barrett, C. J., Light-induced nanostructure formation using azobenzene polymers. *Polymeric Nanostructures and Their Applications 0* **2006**, 1-38.

54. Han, M.; Ichimura, K., Tilt orientation of p-methoxyazobenzene side chains in liquid crystalline polymer films by irradiation with nonpolarized light. *Macromolecules* **2001,** *34* (1), 82-89.

55. Natansohn, A.; Rochon, P., Photoinduced motions in azo-containing polymers. *Chemical Reviews* **2002,** *102* (11), 4139-4176.

56. Hurduc, N.; Donose, B. C.; Macovei, A.; Paius, C.; Ibanescu, C.; Scutaru, D.; Hamel, M.; Branza-Nichita, N.; Rocha, L., Direct observation of athermal photofluidisation in azo-polymer films. *Soft Matter* **2014,** *10* (26), 4640-4647.

57. Yadavalli, N. S.; Loebner, S.; Papke, T.; Sava, E.; Hurduc, N.; Santer, S., A comparative study of photoinduced deformation in azobenzene containing polymer films. *Soft Matter* **2016,** *12* (9), 2593-2603.

58. Galinski, H.; Ambrosio, A.; Maddalena, P.; Schenker, I.; Spolenak, R.; Capasso, F., Instability-induced pattern formation of photoactivated functional polymers. *Proceedings of the National Academy of Sciences* **2014,** *111* (48), 17017-17022.

59. Jeng, R.; Chen, Y.; Kumar, J.; Tripathy, S., Novel crosslinked guest-host system with stable second-order nonlinearity. *Journal of Macromolecular Science—Pure and Applied Chemistry* **1992,** *29* (12), 1115-1127.

60. Kim, D.; Tripathy, S.; Li, L.; Kumar, J., Laser-induced holographic surface relief gratings on nonlinear optical polymer films. *Applied Physics Letters* **1995,** *66* (10), 1166-1168.

61. Rochon, P.; Batalla, E.; Natansohn, A., Optically induced surface gratings on azoaromatic polymer films. *Applied Physics Letters* **1995,** *66* (2), 136-138.

62. Yadavalli, N. S.; Santer, S., In-situ atomic force microscopy study of the mechanism of surface relief grating formation in photosensitive polymer films. *Journal of Applied Physics* **2013,** *113* (22), 224304.

63. Bian, S.; Li, L.; Kumar, J.; Kim, D.; Williams, J.; Tripathy, S., Single laser beam-induced surface deformation on azobenzene polymer films. *Applied Physics Letters* **1998,** *73* (13), 1817-1819.

64. Bian, S.; Williams, J. M.; Kim, D. Y.; Li, L.; Balasubramanian, S.; Kumar, J.; Tripathy, S., Photoinduced surface deformations on azobenzene polymer films. *Journal of Applied Physics* **1999,** *86* (8), 4498-4508.

65. Noga, J.; Sobolewska, A.; Bartkiewicz, S.; Virkki, M.; Priimagi, A., Periodic Surface Structures Induced by a Single Laser Beam Irradiation. *Macromolecular Materials and Engineering* **2017,** *302* (2).

66. Ambrosio, A.; Camposeo, A.; Carella, A.; Borbone, F.; Pisignano, D.; Roviello, A.; Maddalena, P., Realization of submicrometer structures by a confocal system on azopolymer films containing photoluminescent chromophores. *Journal of Applied Physics* **2010,** *107* (8), 083110.

67. Tuma, J.; Lyutakov, O.; Huttel, I.; Slepicka, P.; Svorcik, V., Reversible patterning of poly (methylmethacrylate) doped with disperse Red 1 by laser scanning. *Journal of Applied Physics* **2013,** *114* (9), 093104.

68. Rocha, L.; Păiuş, C.-M.; Luca-Raicu, A.; Resmerita, E.; Rusu, A.; Moleavin, I.-A.; Hamel, M.; Branza-Nichita, N.; Hurduc, N., Azobenzene based

polymers as photoactive supports and micellar structures for applications in biology. *Journal of Photochemistry and Photobiology A: Chemistry* **2014,** *291*, 16-25.

69. Sadovski, O.; Beharry, A. A.; Zhang, F.; Woolley, G. A., Spectral tuning of azobenzene photoswitches for biological applications. *Angewandte Chemie International Edition* **2009,** *48* (8), 1484-1486.

70. Barille, R.; Janik, R.; Kucharski, S.; Eyer, J.; Letournel, F., Photo-responsive polymer with erasable and reconfigurable micro-and nano-patterns: an in vitro study for neuron guidance. *Colloids and Surfaces B: Biointerfaces* **2011,** *88* (1), 63-71.

71. Baac, H.; Lee, J.-H.; Seo, J.-M.; Park, T. H.; Chung, H.; Lee, S.-D.; Kim, S. J., Submicron-scale topographical control of cell growth using holographic surface relief grating. *Materials Science and Engineering: C* **2004,** *24* (1), 209-212.

72. Kollarigowda, R.; Fedele, C.; Rianna, C.; Calabuig, A.; Manikas, A.; Pagliarulo, V.; Ferraro, P.; Cavalli, S.; Netti, P., Light-responsive polymer brushes: active topographic cues for cell culture applications. *Polymer Chemistry* **2017,** *8* (21), 3271-3278.

73. Rianna, C.; Calabuig, A.; Ventre, M.; Cavalli, S.; Pagliarulo, V.; Grilli, S.; Ferraro, P.; Netti, P. A., Reversible holographic patterns on azopolymers for guiding cell adhesion and orientation. *ACS Applied Materials & Interfaces* **2015,** *7* (31), 16984-16991.

74. Koçer, G.; ter Schiphorst, J.; Hendrikx, M.; Kassa, H. G.; Leclère, P.; Schenning, A. P.; Jonkheijm, P., Light-Responsive Hierarchically Structured Liquid Crystal Polymer Networks for Harnessing Cell Adhesion and Migration. *Advanced Materials* **2017**.

75. Rianna, C.; Rossano, L.; Kollarigowda, R. H.; Formiggini, F.; Cavalli, S.; Ventre, M.; Netti, P. A., Spatio-Temporal Control of Dynamic Topographic Patterns on Azopolymers for Cell Culture Applications. *Advanced Functional Materials* **2016,** *26* (42), 7572-7580.

Chapter 2

Dynamic Topographic Pattern Embossed on Cell-Populated Azopolymers by Confocal Microscope Set-Up.*

Abstract.

Topographic signals influence different cell functions such as adhesion, migration and differentiation. Various techniques have been developed to produce topographic patterns on biosurfaces in order to study cell behavior. However, the current understanding of the interplay between cells and topography mainly relies on a static display of signals. Here, we investigated the cell response to dynamic and reversible topographic patterns on azopolymer surfaces. The versatility of laser-based confocal technique is exploited, since it enables to imprint multiple topographic features on azofilms with high resolution. Furthermore, this methodology allows evaluating of cell behavior in real-time. In this study cell-material crosstalk is investigated in a dynamic way by inducing spatio-temporal dynamic topographic changes to cells directly seeded on the substrate, overcoming the limits of static and irreversible *in vitro* systems.

*A part of this project was developed in the group of Prof. M. Riehle, University of Glasgow, Glasgow (UK).

*The work described in this chapter is part of a published article: Rianna, C.; Rossano, L.; Kollarigowda, R. H.; Formiggini, F.; Cavalli, S.; Ventre, M.; Netti, P. A., Spatio-Temporal Control Of Dynamic Topographic Patterns On Azopolymers For Cell Culture Applications. *Advanced Functional Materials* **2016,** *26* (42), 7572-7580.

2.1 Introduction

The extracellular matrix is an active structure, source of the signals that promote, guide and sustain cell functions. These signals can be in the form of biochemical stimuli (fixed proteins or diffusible factors), mechanical stimuli (hard/elastic, soft/compliant or gel-like tissues) and topographical stimuli (fibrils, fibers, pores, meshes, protrusions).[1] In the past decades, the effects of these cues on cell behavior have been extensively investigated and among these signals, topographic cues proved to be effective in controlling cell behavior.[2] *In vivo*, ECM is a network of pores, fibers, ridges and other features of micro or nano-meter sized dimensions, that influence cell fate.[3] The principal techniques used to emboss topographic features on substrates mainly deal with static materials, which do not allow any change in topography once cells are cultured on them.[4-5] However, in an *in vivo* context, extracellular matrix continuously changes its biochemical/biophysical features displaying different signals to cells in a spatio-temporal dependent manner.[6] For this reason, in an *in vitro* context, the development of "dynamic" biomaterials, able to change their topographic features in time and space, is crucial to overcome the limits of physically "static" systems.[7-8] Most of these platforms relied either on irreversible sequential modification of the chemical/physical structure, or on the switching between two reference configurations.[7] In both cases, the effectiveness of these systems is limited since reversibility or multipatterning cannot be readily exploited. Recently, stimulus-responsive materials have been used as "dynamic" supports,[7, 9-10] because they are powerful tools for preparing dynamic cell culture platforms. In particular, a special attention has been focalized on light responsiveness, because light can be precisely localized over a substrate, programmed in time and in space and remotely addressable at a proper wavelength in a biocompatible fashion. Specifically, light-responsive materials containing azobenzene moieties have been shown the inscription of topographic features in dynamic manner because they exhibited a unique and remarkable surface-mass

transport under proper illumination conditions[11] due to a reversible *trans-cis-trans* isomerization process of a special class of azobenzene molecules (the push-pull type such as Poly Disperse Red 1, pDR1).[12-13] Furthermore, using an incoherent or unpolarized light that randomizes the azobenzene molecule orientations, the topographic pattern can be easily erased reestablishing the initial pattern conditions.[14] In this chapter, pDR1 azofilms were used as cell culture supports in order to inscribe topographic patterns with a tight spatio-temporal control of their features. The confocal microscope set-up allowed the inscription of micron and submicron-scale structures on azopolymers for studying cell behavior, in particular, this optical technique enabled to directly induce dynamic topographic cues to live cells at different times or locations and study cell response in a real-time manner.

2.2 Results and Discussions

2.2.1 Pattern Inscription on Azopolymer Substrates

Single photon confocal microscopy was used to emboss precise and complex sub-micrometric patterns on pDR1m thin films. In detail, since the maximum absorption band of our polymer is 467 nm, the laser sources with wavelength values of both 405, 488 and 514 nm were used to induce the continuous *trans-cis-trans* isomerization of pDR1m molecules, hence the resulting surface mass migration.[15-16] The laser beam path can be controlled via software by drawing specific region of interests (ROIs) in which the laser was activated only in the selected regions with a high spatial resolution (nm order). Since topographic patterns were generated by laser-induced mass displacement, it was reasonable to expect that the features would be affected by the processing parameters. For this reason, we performed a systematic study to evaluate the influence of the laser intensity and the dwell time on pattern inscription; in particular we found a relationship of these two parameters with the pattern height. In the first experiment,

we tuned the light intensity, maintaining all other parameters fixed (irradiation with Argon laser at 514 nm for 45 s). As expected, we found that the height increased with increasing the light intensity (Figure 2.1).

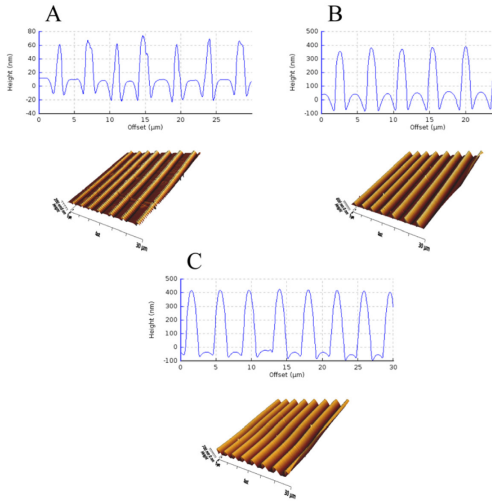

	Intensity [mW]	Height [nm]
A	0,5	65
B	1,3	350
C	2,6	400

Figure 2.1 AFM images of linear pattern tuning the light intensity. A) 0.5 mW, B) 1.3 mW and C) 2.6 mW.

In the second case, we varied the time course only (Argon laser at 514 nm with 1.3 mW of laser intensity) (Figure 2.2).

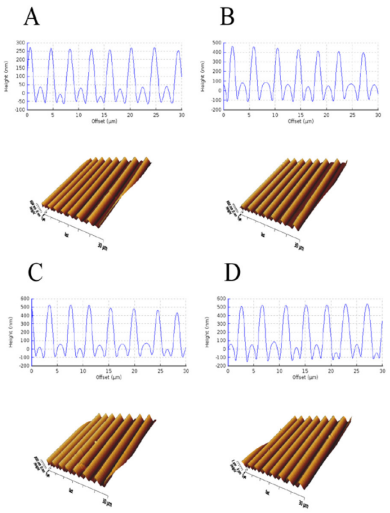

	Time course [sec]	Height [nm]
A	15	250
B	30	450
C	45	500
D	60	550

Figure 2.2 AFM images of linear pattern tuning the laser intensity. A) 15 s, B) 30 s, C) 45 s and D) 60 s.

The height of linear pattern increased about 300 nm until 30 s of irradiation, after this time, the difference in height value changed about 50 nm only.

The peculiarity of the confocal microscope set-up enabled us to produce complex topographies by simply changing the shape and the direction of the ROIs. In our experiments, rectangular ROIs were used to emboss linear gratings on azofilms, irradiating the sample with laser at different wavelengths. As a first example, the substrates were irradiated for 30 s with Argon laser at 514 nm (laser intensity of 1.3 mW). Furthermore, a sort of grid pattern was obtained by just scanning the laser in perpendicular parallel ROIs (Figure 2.3).

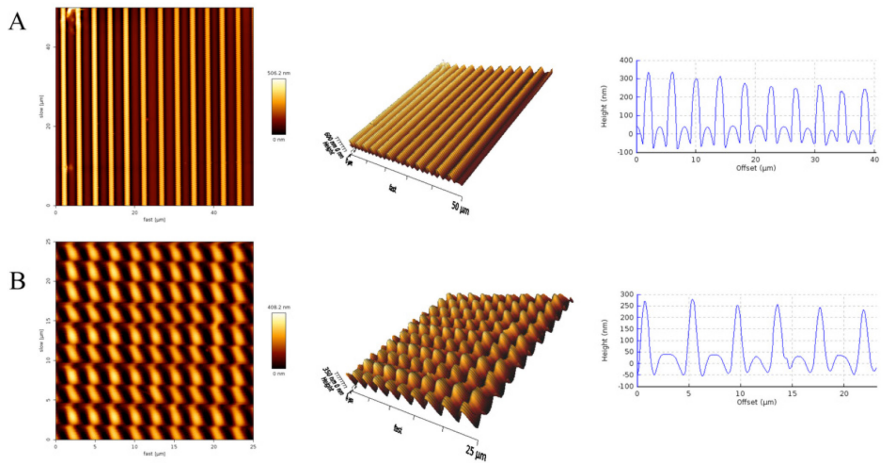

Figure 2.3 AFM image of embossed pattern on pDR1m with Argon laser at 514 nm in 30 s: 2D image, 3D image and cross section profile of A) linear pattern and B) grid pattern.

In the other experiments, rectangular ROIs were used to produce parallel gratings on azofilms, by irradiating the sample for 30 s with Argon laser at 488 nm (laser intensity of 1.3 mW) (Figure 2.4 A) and diode laser at 405 nm (laser intensity of 1.4 mW) (Figure 2.4 B). These patterns differed in the size of the embossed topographies.

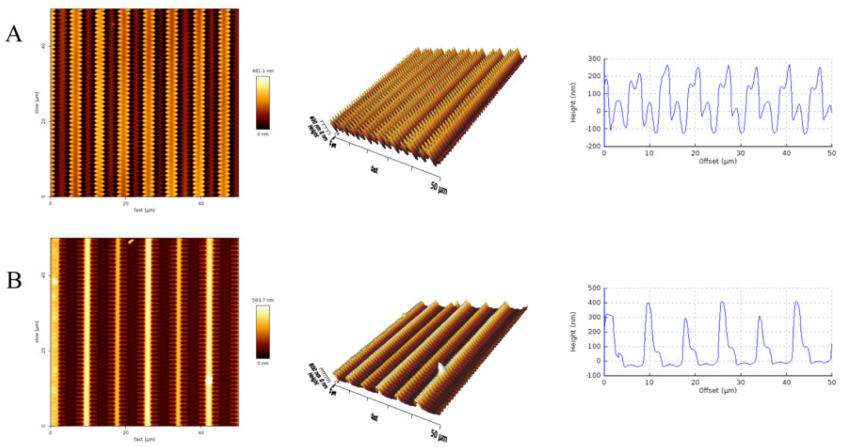

Figure 2.4 AFM images of linear embossed pattern on pDR1m: 2D image, 3D image and cross section profile of A) irradiation with Argon laser at 488 nm for 30 s and B) irradiation with diode laser at 405 nm for 30 s.

The versatility of the confocal technique made it possible to produce topographic pattern with different methods. Therefore, the possibility to inscribe similar linear features using masks was also investigated. In our experiments, masks were placed between the light source and the azofilms and the samples were irradiated for 60 s at 405 nm (laser intensity of 1.4 mW).

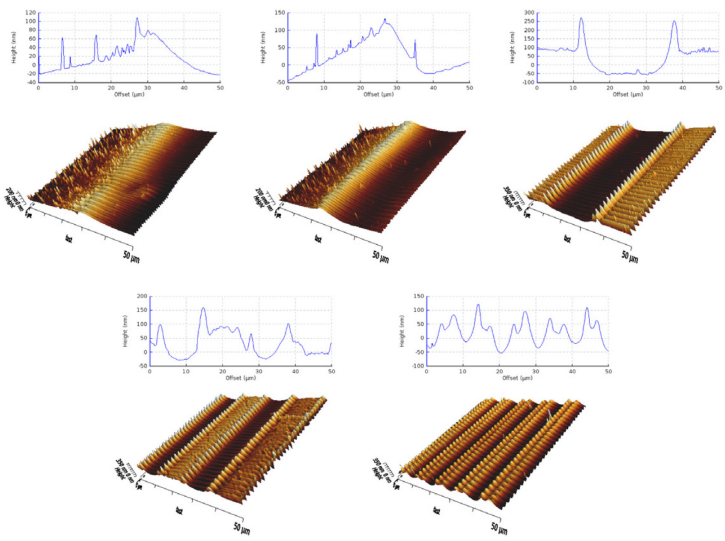

Figure 2.5 AFM image of embossed pattern on pDR1m using masks with diode laser at 405 nm irradiating for 60 s.

The previous image (Figure 2.5) shows a double topography for each topographic pattern embossed. The first according to the direction and the size of the vertical mask with micrometric dimension and the second due to the nanometric laser scanning lines. Remarkably, all the patterns were stable in time and in water, but mass migration can also be a reversible phenomenon.[11] Patterns could be removed by heating the sample above the polymer glass transition temperature (Tg = 82 °C) as well as by using circularly polarized light or incoherent and unpolarized light in dry conditions.[17] Furthermore, the topographic features were erased with the use of an incoherent and unpolarized light of a mercury lamp, mounted on the confocal set-up. In these conditions the height of pattern declined by 200 nm after 60 s of illumination (Figure 2.6).

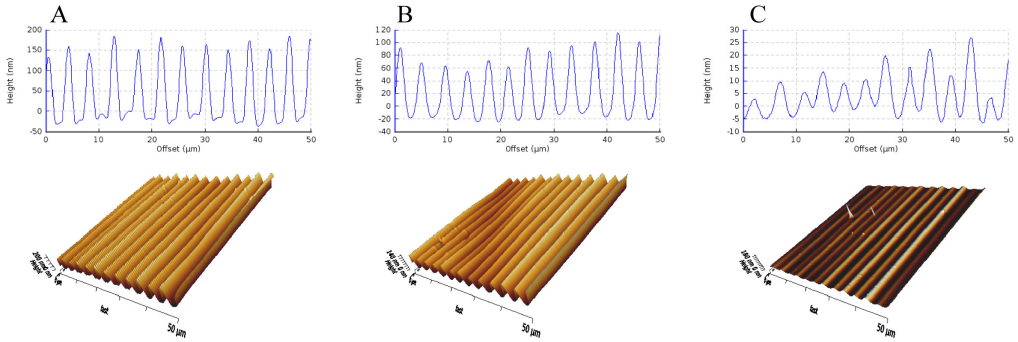

Figure 2.6 AFM images of linear pattern. A) Before illumination. After illumination using a mercury lamp for B) 30 s, C) 60 s.

In summary, the major peculiarity of the confocal technique, described in this section, is related to the possibility to inscribe different topographic features on azosubstrates by varying the condition of the inscription parameters and the shape/size of the ROIs used for laser scanning. Finally, another important characteristic of such azofilms, which is the reversibility of the mass transport, could also be investigated applying the confocal set-up. Indeed, the possibility to reverse to initial topographic conditions is an important issue in the field of "dynamic" cell-instructive materials.

2.2.2 Effect of Static Topographic Pattern on Epithelial Cell Behavior

The literature reports that Madin-Darby canine kidney (MDCK) cells are very susceptible to substratum guidance.[18] Therefore, we used this cell line as a reliable model to investigate whether the geometrical features of the laser-inscribed patterns were effective in altering MDCK adhesion and orientation. In detail, we found that epithelial cells cultivated on linear patterns with different pitch perceived the topographic features and changed their shape accordingly. In fact, cells were aligned on linear gratings (Figure 2.7 A-B-C) and they had a round shape on grid patter (Figure 2.7 D).

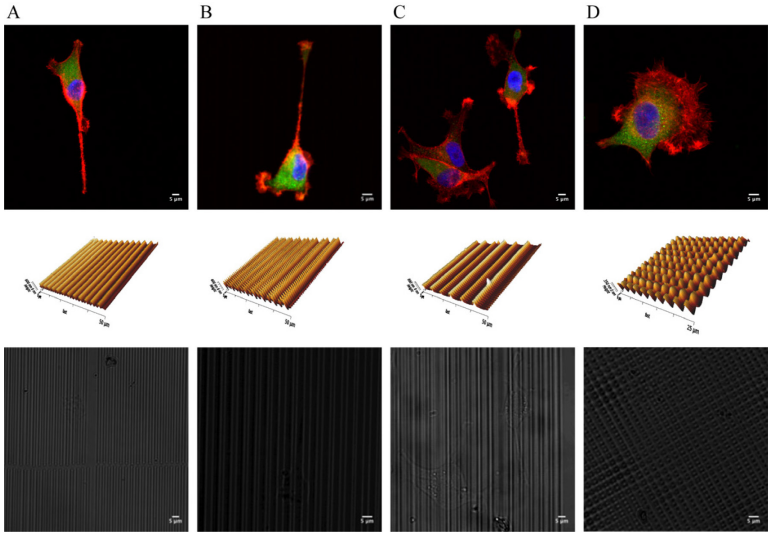

Figure 2.7 Cell orientation on confocal-induced pDR1m patterns. (Upper panel) Fluorescent images of fixed MDCK cells on pDR1m patterns. Cell cytoskeleton is stained with phalloidin (red), focal adhesions are immunostained for vinculin (green) and nuclei are stained with draq-5 (blue). Scale bars are 5 µm. AFM images and transmission images of topographic patterns (Middle and lower panel, respectively). Cells were seeded on A) linear pattern obtained with laser at 514 nm, B) linear pattern obtained with laser at 488 nm, C) linear pattern obtained with laser at 405 nm and D) grid pattern obtained with laser at 514 nm.

Generally, epithelial cells were organized in colonies, whose shape differed from one sample to another and the cells that were part of colonies reacted differently than those that were still isolated single cells.[18] It is known that when epithelial cells are cultured at a single-cell level, they behave like mesenchymal cells.[19] In detail, the so-called epithelial-mesenchymal transition (EMT) is a biologic process that allows a polarized epithelial cell, to undergo multiple biochemical changes that

enable it to assume a mesenchymal cell phenotype, which includes enhanced migratory capacity, invasiveness, elevated resistance to apoptosis and greatly increased production of ECM components. On the other hand, when cells are cultured at multicellular level, they behave like epithelial cells.[19] For this reason, we evaluated the nuclei characteristics as a function of cell number, by seeding them on linear gratings embossed using Argon laser at 514 nm (Figure 2.8) in order to evaluate a different cell response. The epithelial cells in contact with linear gratings maintained the same nuclei area throughout the entire experiment.

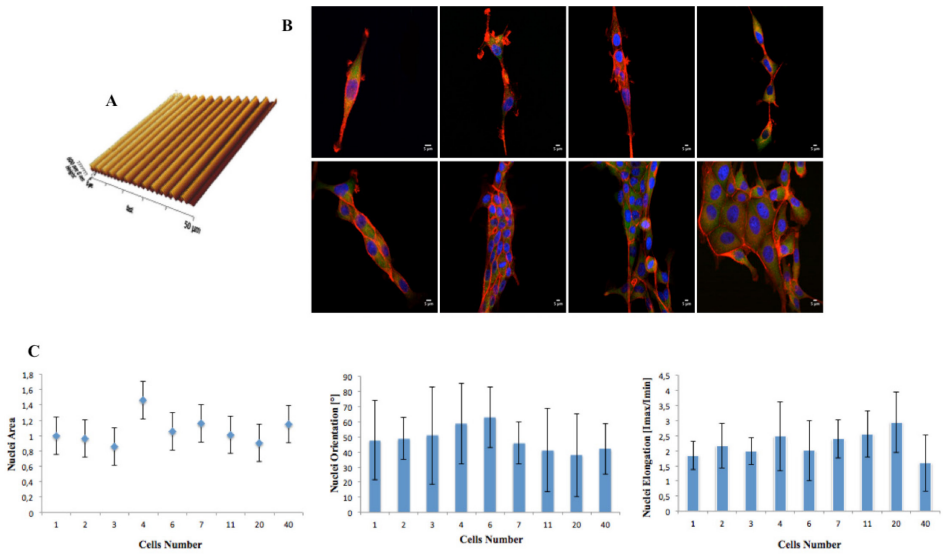

Figure 2.8 A) AFM image of linear pattern embossed using Argon laser at 514 nm. B) Fluorescent images of fixed MDCK cells on linear patterns. Cell cytoskeleton is stained with phalloidin (red), focal adhesions are immunostained for vinculin (green) and nuclei are stained with draq-5 (blue). Scale bars are 5 µm. C) Quantitative analysis of nuclei area, orientation and elongation. Bars refer to the standard deviation. Linear pattern is parallel to the vertical axis (i.e., 90 °).

Furthermore, we observed that the orientation and elongation of MDCK cells to linear topographies were dependent on whether the cell was isolated or part of a colony. In fact, the experimental results evidenced that cells responded to the underlying topography when they began to form little colonies. Precisely, the nuclei were randomly oriented and much less elongated when they were in bigger clusters, in which the cell-cell signaling between neighboring cells increased. This result can be explained by presuming that cell-cell contacts play a key role in

collective behavior of such type of cells.[19] In detail, the difference in the reaction of isolated MDCK cells compared to those in colonies may be due to a number of factors. Cell-cell interactions produce forces that override the cell-material crosstalk by influencing the cell alignment on topographic features. In fact, colonies of endothelial cells appeared to be little affected by the substratum characteristics. The phenomenon of contact-induced spreading of epithelial cells may play a part in or be entirely responsible for the differences between isolated MDCK cells and those in colonies.[18] Also, as a demonstration of the versatility of the confocal set-up, mask-patterned substrates have been used for studying the influence of a static regular topography on cell response (Figure 2.9).

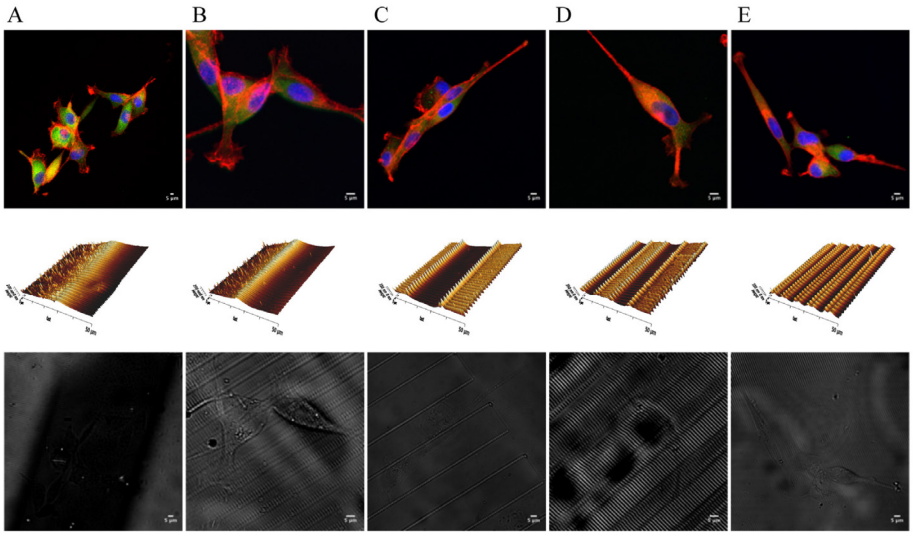

Figure 2.9 Cell orientation on mask-induced pDR1m patterns. (Upper panel) Fluorescent images of fixed MDCK cells on pDR1m patterns. Cell cytoskeleton is stained with phalloidin (red), focal adhesions are immunostained for vinculin (green) and nuclei are stained with draq-5 (blue). Scale bars are 5 μm. AFM and transmission images of topographic patterns (Middle and lower panel, respectively).

In this set of samples, epithelial cells perceived an orthogonal nanometric linear topography, caused by the scansion laser and perpendicular to the micrometric one and preferred to follow these nanometric gratings. Surface modifications induced on azopolymers are, in principle, reversible. In particular, an incoherent and unpolarized light beam of a mercury lamp can be used to erase the patterns because the light provokes a randomization of azobenzene molecules. Starting from this

observation, we irradiated a cell-populated linear pattern, embossed using argon laser at 514 nm, for 30 s with the mercury lamp. However, cells were still vital, migrated over the substrate and were fixed after 24 h from erase process (Figure 2.10).

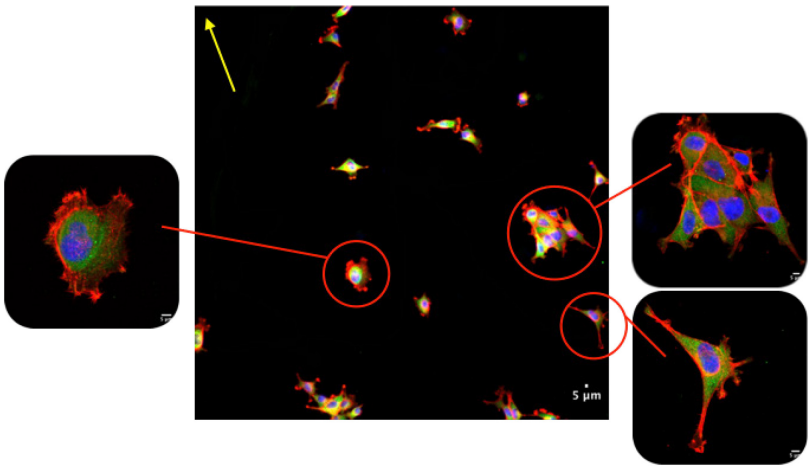

Figure 2.10 Confocal images of MDCK cells cultivated on a linear pattern exposed to incoherent and unpolarized light. Yellow arrow shows the original pattern direction. Cell cytoskeleton is stained with phalloidin (red), focal adhesions are immunostained for vinculin (green) and nuclei are stained with draq-5 (blue). Scale bars are 5 µm.

The epithelial cells lost completely cell orientation after erasing process and did not have a preferential direction of polarization. This set-up of experiments demonstrated the potential of confocal microscope because it let us the modulation of topographic features on azopolymer substrates to control and guide cell behavior.

2.2.3 Evaluating Cell Response on Dynamic Topographic Patterns

As already mentioned above, the innovative confocal technique describe here, is adaptable to the cell environment conditions and the laser intensity power is suitable for dynamic real-time experiments with cells. In fact, the microscope set-up allows the pattern feature alteration in the presence of cells without affecting their viability. Initially, we evaluated the capability of NIH-3T3 fibroblasts to respond to dynamic topographic patterns. It is know that fibroblasts cells respond

to local variations in topography by altering their morphology and migration, in particular, variable substratum topography can result in distinct cell compartments, such cytoskeleton and focal adhesion reorganization. Furthermore, fibroblasts cultured as monolayers retain most of the properties displayed by single cells[20] and their tendency to remain isolated cells allowed a better understanding of cellular-dynamic topographies interactions. Figure 2.11 shows the inscription of a linear grating in presence of live fibroblast cells, without affecting its viability and motility.

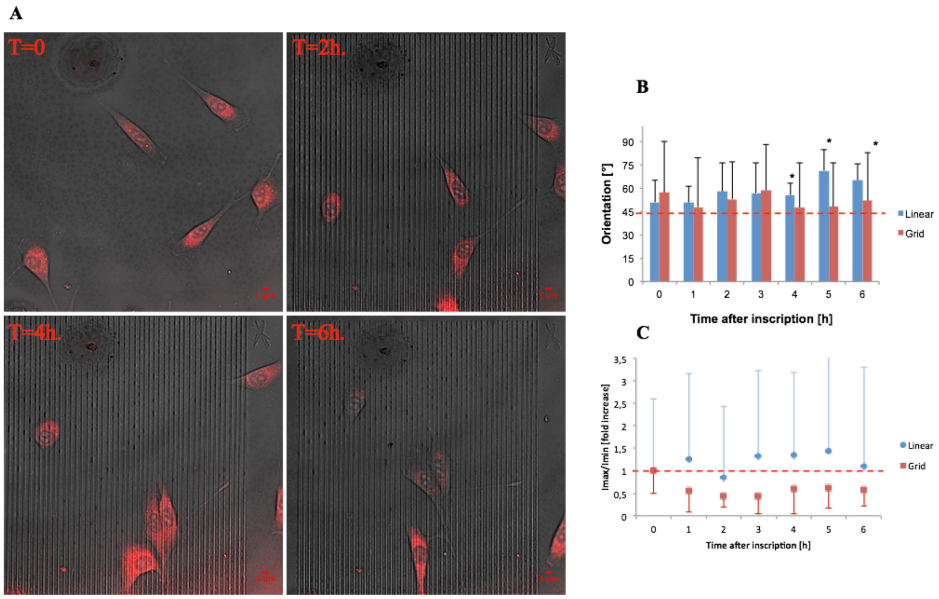

Figure 2.11 A) Cell alignment on PDR1 substrates in real-time. Cells were stained with Deep Red. Scale bars are 5 µm. B) Quantitative analysis of time-changes in cell orientation on the linear pattern (blue columns) and grid patterns (red columns). Linear pattern is parallel to the vertical axis (i.e., 90 °). The asterisk indicates significant differences with respect to the nonpatterned case at time 0 ($p < 0.05$). Bars refer to the standard deviation. C) Quantitative analysis of cell elongation index on the linear patterns (blue circles) and grid (red squares). Variations are reported as fold changes with respect to the initial nonpatterned case (red line set at 1). Data points referring to the grid case from 1h onward are significantly different than 1 ($p < 0.05$). Adapted with permission form.[21] Advanced Functional Materials.

Fibroblasts were stained with a live staining, Deep Red Cell Tracker TM, in order to observe their shape and behavior in real-time. The choice of Deep Red was due to the need to use a dye that absorbs at wavelengths of far red, so outside the absorption spectrum of the underlying azobenzenes. In this way, it is possible separate the wavelength of laser beam used for pattern inscription (405-514 nm)

from those used for imaging of cell shape (650-700 nm). In the early period after inscription, cells maintained the original orientation and shape. However, at longer times, the cells reacted to the underlying topography by changing its orientation. Successively, the time-changes in cell orientation, elongation and area after embossing a linear pattern or a grid, using an Argon laser at 514 nm, on a cell-populated flat sample, were evaluated for a larger set of cells. Initially, cells were randomly oriented on both patterns, however, after 5 hours from pattern inscription, fibroblasts on the linear grating begun to align along the groove direction, while, cells on the grid did not show a preferential direction of orientation during the entire experiment (average orientation of ≈ 45 °). In this experiment, time-changes in cell elongation are reported as fold changes with respect to the initial, nonpatterned case. NIH-3T3 fibroblasts in contact with the linear grating maintained the same elongation level throughout the experiment. Conversely, cells on the grid acquired a significantly lower elongation with respect to the initial nonpatterned case, within 1 hour after the pattern inscription and maintained this value for the entire experiment. Regarding cell area analysis, we did not observe significant changes between cells on linear and grid patterns with respect of the flat substrate that suggest that changes in cell orientation and elongation result from a redistribution of cell area rather than an increased or polarized spreading.[21]

2.2.4 On-Off and Time-Spatial Control of Dynamic Topographic Pattern Inscription

The confocal microscope technique enables the inscription of single or multiple patterns. However, reversibility is a crucial aspect within the context of dynamic signal presentation in order to mimic the remodeling of natural ECM and for this reason we made an experimental campaign aimed at switching off the topographic signal in presence of live cells. Using an incoherent and unpolarized light of a mercury lamp, mounted on the confocal set-up, allowed the erasure of topographic patterns on cell-populated pDR1m. However, these incoherent light exposure

generates bubbles with micrometer dimensions on the azosurface, in presence of aqueous media.[21] To overcome this problem, we removed the cell couture medium during pattern erasure process in order to have a better control in the erasing procedure and to avoid the formation of bubbles. This method did not affect cell viability. As a proof of concept, in Figure 2.12, we showed the feasibility of writing-erasing-rewriting different topographic patterns on fibroblast-populated azofilm.[21]

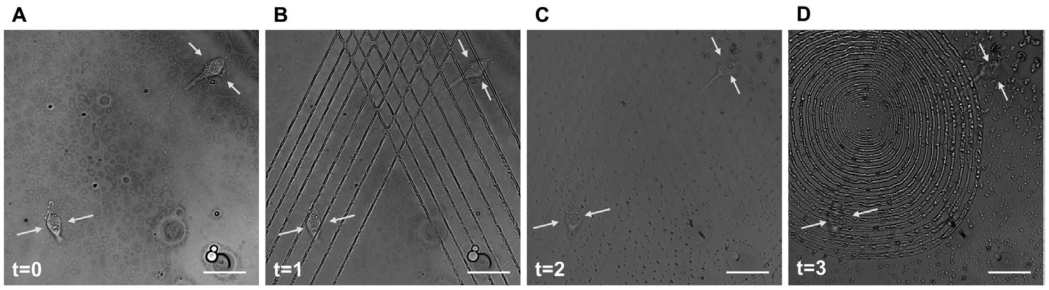

Figure 2.12 Writing-erasure process. Confocal images of A) two cells on flat pDR1m, B) same location after first pattern inscription with 514 nm Argon laser during 30 s, C) pattern erasure by employing unpolarized and incoherent light for 60 s after removing the medium, D) second pattern inscription with 514 nm Argon laser during 30 s. Images were collected at time zero (before patterning) and later at three different time points (t = 1, 2 and 3). White arrows show cell nuclear regions during the entire process. Scale bars are 20 μm. Adapted with permission form.[21] Advanced Functional Materials.

A further peculiarity of the confocal technique consists in enabling multiple pattern inscriptions on the same platform simultaneously, so that isolated cells can be expose to different patterns in real-time. Two different patterns could be embossed on cell-populated azosubstrate to evaluate different cell response simultaneously. After 45 min additional modifications to the previous patterns were performed, demonstrating that the process enables a fine control of the spatio-temporal features of the patterning (Figure 2.13).[21] The possibility to imprint and erase several topographic patterns on azopolymer films with an easy and versatile method may pave the way to an in-depth investigation of complex processes involved in cell-material interaction, such as contact guidance and mechanotransduction phenomena, actively mimicking *in vitro* what potentially happens *in vivo*.

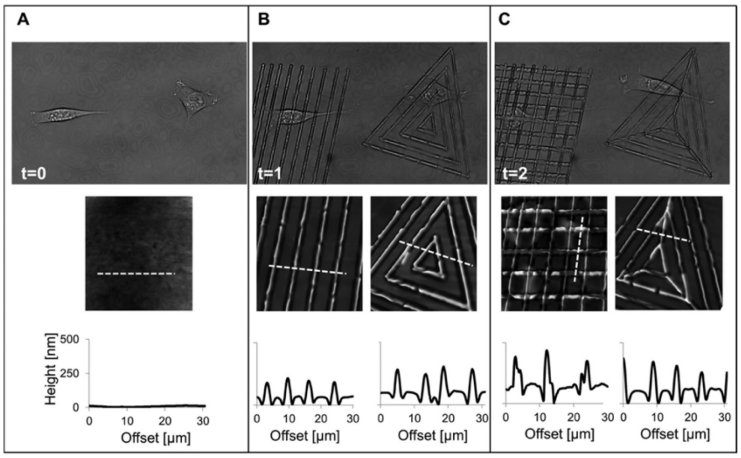

Figure 2.13 Confocal images of A) two cells seeded on flat pDR1m (time zero), B) same location after two different pattern inscriptions and C) after second patterning. AFM images show topography of substrates and cross-section profiles present pattern size at the position marked with a white dashed line on the AFM figures. Adapted with permission form.[21] Advanced Functional Materials.

2.3 Conclusions

The confocal set-up is an innovative optical technique for imprinting and modifying large-scale topographic patterns on pDR1m-substrates. This pattern can be easily inscribed by controlling the single laser beam activation and position. Furthermore, patterns can be erased, under dry conditions, using an incoherent and unpolarized light of a mercury lamp. In particular, the confocal technique is a promising strategy for real-time experiments because, in the confocal set-up, illumination exposure time and laser intensity power did not affect cell viability. Several patterns have been produced on azopolymer films with submicron scale resolution. Initially, epithelial cell response was evaluated on "static" topographic signals revealing that the pattern dimensions have an important influence in cell orientation. Overcoming the limit of conventional "static" cell culture platforms, the confocal technique has a great impact in the investigation of cell-topography interactions in time, thanks to the versatile dynamic presentation of topographic signals. This technique aimed at modifying the topography of cell-populated azofilms with a tight control on dynamic changes, spatial resolution and surface

positioning. Fibroblasts seeded on azofilms responded to such “dynamic” topographies, modifying their morphology and orientation in time. These preliminary results demonstrated that this innovative method might paves the way to study cell behavior in a dynamic and biomimetic way, owing to the versatility of optical set-up and the unique properties of the azobenzene moieties.

2.4 Experimental Section

2.4.1 General Materials

Poly(Disperse Red 1 methacrylate) (pDR1m), all solvents, TRITC phalloidin were provided by Sigma. Cell Tracker Deep Red was supplied from Thermo Scientific, anti-vinculin monoclonal antibody was provided from Chemicon (EMD Millipore), Alexa Fluor 488 conjugated goat antimouse antibody and Deep Red Anthraquinone 5 (DRAQ-5) were purchased from Abcam. Fibroblast (NIH-3T3) and Madin-Darby Canine Kidney (MDCK) cells were purchased from ATCC.

2.4.2 Sample Preparation

pDR1m was dissolved in chloroform (5% w/v) and then spins coated onto a glass coverslip in order to produce thin film of pDR1m. In detail, 12 mm diameter circular cover glasses were washed in acetone, sonicated three times for 15 min and then dried on a hot plate prior to spin coating process. The pDR1m solution was spun over the cover glass by using a Laurell spin coater at 1500 rpm and a profilometer was used to monitor the thickness of the polymer film (about 300 nm).

2.4.3 Micropattern Inscription

A SP5 laser scanning confocal microscope (Leica Microsystems, Germany) and a LSM 780 confocal microscope (Zeiss, Germany) were used to emboss different

topographic patterns on pDR1m substrates. A JPK NanoWizard II atomic force microscopy (AFM) (JPK Instruments, Germany) was used to monitor and visualize the surface topography of pDR1m films. An Axio Observer Z1 microscope (Zeiss, Germany) was combined to the AFM to control tip and sample position. Silicon Nitride tip (MLCT, Bruker, USA) with a spring constant of 0.01 Nm^{-1} was used in contact mode, in air, at room temperature.

2.4.4 Cell Culture

NIH-3T3 fibroblast and MDCK epithelial cells were cultured in low and high glucose DMEM (Dulbecco's Modified Eagle Medium), respectively and incubated at 37 °C in a humidified atmosphere of 95% air and 5% CO_2. pDR1m substrates were sterilized under UV light for 30 min and subsequently cells were seeded on them without any additional treatment.

2.4.5 Cell Staining

In case of static experiments on patterned structures, after 24 h from cell seeding, cells were fixed with 4% paraformaldehyde for 15 minutes and then permeabilized with 0.1% Triton X-100 in PBS for 3 min. The actin filaments were stained with TRITC-phalloidin; samples were incubated for 30 min at room temperature in the phalloidin solution (dilution 1:200). For focal adhesions staining, cells were incubated in an anti-vinculin monoclonal antibody solution (dilution 1:200) for 2 h at 20 °C and successively marked with Alexa Fluor 488 conjugated goat anti-mouse antibody (dilution 1:1000) for 30 min at 20 °C. Finally cells were incubated for 15 min at 37 °C in a Draq-5 solution (dilution 1:1000) to stain nuclei. The laser lines used were 488 nm (vinculin), 543 nm (actin) and 633 nm (nuclei). The emissions were collected in the ranges of 500-530, 560-610 or 650-720 nm, respectively.

2.4.6 Dynamic Topographic Pattern Inscription

In the case of real-time pattern inscription on fibroblast-populated azopolymer films, cells were seeded on the flat spin-coated film 24 hours prior to pattern inscription. Once at the microscope, several ROIs were drawn and selectively irradiated with 514 nm Argon light for 30 s (a 40X/1.1 water immersion microscope objective was used as focusing lens). The laser intensity corresponded to 1.3 mW and the scan speed was of 400 Hz. On MDCK cell-populated films, ROIs were irradiated with diode light at 405 nm for 30 s and with Argon laser at 488 nm for 30 s (a 50X/0.55 dry microscope object was used as focusing lens). The laser intensity was 1.4 mW and 1.5 mW, respectively. In the case of static pattern inscription on MDCK-populated azofilms, a mask was positioned on each substrate, irradiating with diode at 405 nm for 1 min (a 20X/1.0 dry microscope object was used as focusing lens). The laser intensity was 1.4 mW.

2.4.7 Live-Cell Staining

Living cells were stained with Cell Tracker Deep Red (Thermo Fisher Scientific). A stock solution of the dye was prepared in DMSO (10^3 μM); 2 μL of this solution was diluted with serum free medium (final volume of 1 mL). A SP5 confocal microscope was used to collect living cell images and videos. The dye was excited at 633 nm and emissions were collected in the range of 650-700 nm.

2.4.8 Analysis of Cell Orientation and Elongation

In the case of static experiments on patterned structures, information about nuclei orientation and elongation was obtained by analyzing an immunofluorescence staining of cells. In the case of dynamic experiments on patterned structures, information on cell orientation and elongation was obtained by analyzing a set of single isolated cells, stained with a vital fluorescent dye and images at different times after embossing the linear pattern or the grid on a cell-populated flat sample.

The analyzed set of cells came from three different experiments carried out in analogous conditions, form different patterns inscribed in different regions of the samples. Cell elongation was assessed from images of Cell Tracker Deep Red stained cells and analyzed with the MomentMacroJ version 1.3 script (hopkinsmedicine.org/fae/mmacro.htm). The principal moments of inertia (i.e., maximum and minimum) were evaluated and cell elongation index was defined as the ratio of the principal moments (Imax/Imin). High values of Imax/Imin identify elongated cells. Moreover, cell orientation was defined as the angle that the principal axis of inertia formed with a reference axis. The reference axis was considered as the x-axis. Statistical significance was assessed through t-test (run in Matlab) with level of significance $p < 0.05$.

2.5 References

1. Ventre, M.; Netti, P. A., Engineering cell instructive materials to control cell fate and functions through material cues and surface patterning. *ACS Applied Materials & Interfaces* **2016,** *8* (24), 14896-14908.

2. Hamilton, D. W.; Oates, C. J.; Hasanzadeh, A.; Mittler, S., Migration of periodontal ligament fibroblasts on nanometric topographical patterns: influence of filopodia and focal adhesions on contact guidance. *PLoS One* **2010,** *5* (12), e15129.

3. Flemming, R. G.; Murphy, C. J.; Abrams, G. A.; Goodman, S. L.; Nealey, P. F., Effects of synthetic micro- and nano-structured surfaces on cell behavior. *Biomaterials* **1999,** *20* (6), 573-88.

4. Bettinger, C. J.; Langer, R.; Borenstein, J. T., Engineering substrate topography at the micro-and nanoscale to control cell function. *Angewandte Chemie International Edition* **2009,** *48* (30), 5406-5415.

5. Yao, X.; Peng, R.; Ding, J., Cell–material interactions revealed via material techniques of surface patterning. *Advanced Materials* **2013,** *25* (37), 5257-5286.

6. Wu, M.; Fannin, J.; Rice, K. M.; Wang, B.; Blough, E. R., Effect of aging on cellular mechanotransduction. *Ageing Research Reviews* **2011,** *10* (1), 1-15.

7. Davis, K. A.; Burke, K. A.; Mather, P. T.; Henderson, J. H., Dynamic cell behavior on shape memory polymer substrates. *Biomaterials* **2011,** *32* (9), 2285-2293.

8. Rianna, C.; Calabuig, A.; Ventre, M.; Cavalli, S.; Pagliarulo, V.; Grilli, S.; Ferraro, P.; Netti, P. A., Reversible holographic patterns on azopolymers for guiding cell adhesion and orientation. *ACS Applied Materials & Interfaces* **2015,** *7* (31), 16984-16991.

9. Le, D. M.; Kulangara, K.; Adler, A. F.; Leong, K. W.; Ashby, V. S., Dynamic Topographical Control of Mesenchymal Stem Cells by Culture on Responsive Poly (ϵ-caprolactone) Surfaces. *Advanced Materials* **2011,** *23* (29), 3278-3283.

10. Ng, C. C. A.; Magenau, A.; Ngalim, S. H.; Ciampi, S.; Chockalingham, M.; Harper, J. B.; Gaus, K.; Gooding, J. J., Using an electrical potential to reversibly switch surfaces between two states for dynamically controlling cell adhesion. *Angewandte Chemie International Edition* **2012,** *51* (31), 7706-7710.

11. Yager, K. G.; Barrett, C. J., Light-induced nanostructure formation using azobenzene polymers. *Polymeric Nanostructures and Their Applications 0* **2006**, 1-38.

12. Barrett, C.; Natansohn, A.; Rochon, P., Cis-trans thermal isomerization rates of bound and doped azobenzenes in a series of polymers. *Chemistry of Materials* **1995,** *7* (5), 899-903.

13. Seki, T.; Sekizawa, H.; Ichimura, K., Non-linear characteristics of the photoinduced deformation in azobenzene-containing monolayers at the air-water interface. *Polymer Journal* **1999,** *31*, 1079-1082.

14. Han, M.; Ichimura, K., Tilt orientation of p-methoxyazobenzene side chains in liquid crystalline polymer films by irradiation with nonpolarized light. *Macromolecules* **2001,** *34* (1), 82-89.

15. Bian, S.; Li, L.; Kumar, J.; Kim, D.; Williams, J.; Tripathy, S., Single laser beam-induced surface deformation on azobenzene polymer films. *Applied Physics Letters* **1998,** *73* (13), 1817-1819.

16. Ambrosio, A.; Camposeo, A.; Carella, A.; Borbone, F.; Pisignano, D.; Roviello, A.; Maddalena, P., Realization of submicrometer structures by a confocal system on azopolymer films containing photoluminescent chromophores. *Journal of Applied Physics* **2010,** *107* (8), 083110.

17. Kim, D.; Tripathy, S.; Li, L.; Kumar, J., Laser-induced holographic surface relief gratings on nonlinear optical polymer films. *Applied Physics Letters* **1995,** *66* (10), 1166-1168.

18. Clark, P.; Connolly, P.; Curtis, A.; Dow, J.; Wilkinson, C., Topographical control of cell behaviour: II. Multiple grooved substrata. *Development* **1990,** *108* (4), 635-644.

19. Kalluri, R.; Weinberg, R. A., The basics of epithelial-mesenchymal transition. *The Journal of Clinical Investigation* **2010,** *120* (5), 1786.

20. Kim, D.-H.; Han, K.; Gupta, K.; Kwon, K. W.; Suh, K.-Y.; Levchenko, A., Mechanosensitivity of fibroblast cell shape and movement to anisotropic substratum topography gradients. *Biomaterials* **2009,** *30* (29), 5433-5444.

21. Rianna, C.; Rossano, L.; Kollarigowda, R. H.; Formiggini, F.; Cavalli, S.; Ventre, M.; Netti, P. A., Spatio-Temporal Control of Dynamic Topographic Patterns on Azopolymers for Cell Culture Applications. *Advanced Functional Materials* **2016,** *26* (42), 7572-7580.

Chapter 3

Study of Cell Behavior on Photo-Responsive Surfaces with Modular Circular Topography.*

Abstract.

In the human body, cells are constantly exposed to physical signals provided by the extracellular microenvironment. Many cell types developed an exquisite sensitivity to these signals; they integrate and transform them into biological responses. For instance, the growth of several biological tissues is known to be controlled in part by local geometric features, such as the curvature of the tissue interface. Topographic cues can affect various aspects of cell behavior including adhesion, spreading, alignment, morphological variations and changes in gene expression. In this chapter, we present a real-time investigation of fibroblast cells behavior on azopolymer substrates with distinct modular circular topographies. The innovation of proposed technique is the dynamic presentation of topographic cues to the cell, by harnessing the versatility of confocal microscope set-up and the unique properties of the azobenzene moieties.

*The work described in this Chapter is a part of a manuscript in preparation. L. Rossano, C. Cimmino, M. Ventre, S. Cavalli and P. A. Netti: "Study of Cell Behavior on Photo-Responsive Surfaces with Modular Circular Topography".

3.1 Introduction

Geometrical properties of the cell environment play an important role as regulators of cell fate.[1-3] In early studies, patterned substrates with various geometries have been used to investigate the relevance of cell behavior and the influence of substrate geometries on stress fibers and focal adhesion organization.[4-5] In fact, it is known that when cells are seeded on patterned substrates, they align, grow or migrate along the topographic features and this phenomenon is known as "contact guidance" and may vary for different cell types.[6-8] Recently, a growing number of reports demonstrated that the substrate shapes included an elaborate range of curvatures, smooth and sharp corners and linear geometries could influence cell behavior, not only in terms of adhesion, migration[9] and alignment,[10] but also in terms of differentiation[11] and expression of stemness markers.[12] For example, concentric microgrooved substrates with different groove widths and depths and precise surface patterns served effectively in demonstrating that the topographical cues regulate pre-osteoblastic cell alignment, distribution and directional mineralization for bone tissue engineering applications.[13] In another recent important report, cancer stem cells (CSCs) were shown to exhibit higher carcinogenicity expression if seeded on circular topography. In particular, interfacial geometry was supposed to trigger a general mechanism for the regulation of cancer-cell state, analyzing how cancer cell could also exploit geometry.[14] Moreover, Zhang *et al.* have demonstrated that a specific curvature induces optimal circumferential alignment of collective vascular smooth muscle cells (SMCs). They found a significant down-regulation of actin expression after the cells became confluent and circumferentially aligned.[15] However, a well understanding of how the curvature of the surface is sensed by cells and how it influences their functions is still missing. Yet, it appears more and more evident the importance of exploring also surface geometry as a cell-instructive material parameter for cell guidance. In this respect, a systematic study of the cell

interaction with controlled substrate curvatures at single-cell-level is still lacking. In this work, Poly (Disperse Red 1 methacrylate) (pDR1m) was used to fabricate dynamic non-linear topographic features on azofilms. In particular, relying on the versatility and accuracy of the confocal microscopy to control laser beam path, complex circular and concentric topographies were produced. In our experiments, NIH-3T3 fibroblasts were used as a model cell line to carry out single cell analysis, since they are easy to culture and show a relatively good response to topographic stimuli. Real-time as well as immunofluorescence imaging allowed to study in time the morphology and the orientation of cells in contact with different circular types of patterns. Mechanical properties also provided useful information on cell state on these modular circular topographies.

3.2 Results and Discussions

3.2.1 Circular Pattern Inscription

The confocal technique enables the inscription of different topographic patterns on cell-populated substrates, by changing the size and the dimensions of geometric features, produced by the confocal software, called region the interest (ROIs), which let us to carefully control the activation and the position of laser beam. In detail, the maximum absorption band of our polymer, pDR1m, is 467 nm, so the wavelengths at 514 nm was chosen to inscribe the topographic features on azosubstrates, obtaining the continuous isomerization of azobenzenes molecules and consequentially the known process of surface mass migration.[16] Negligible topographic modifications were observed using laser at 405 nm. Similarly, a wavelength of 633 nm did not affect azopolymer surface. Since it is well recognized that the 514 nm wavelength is not harmful for living system and moreover it do not affect cell viability,[10] we drew circumferential ROIs with the microscope controlling software and the sample was irradiated for 45 seconds with

Argon laser (514 nm, 1.3 mW laser intensity, 400 Hz scan speed). Furthermore, circular patterns of several dimensions were embossed by modulating the micrometric ROIs distance. In order to study the cell behavior on a circular pattern, three models of different sizes were made (Figure 3.1). These topographic models differed for height and groove dimensions. The first type of circular pattern had a height of 320 nm and a crest-to-crest groove distance of 5 µm (Figure 3.1 A). Then, concentric ROIs at a greater distance were employed to produce other circular features. The second pattern had a height of 400 nm and grooves with crest-to-crest distance of 10 µm (Figure 3.1 B). The third pattern was made using concentric ROIs at even greater distance. A pattern with crest-to-crest groove distance of about 15 µm and a height of about 350 nm was obtained (Figure 3.1 C).

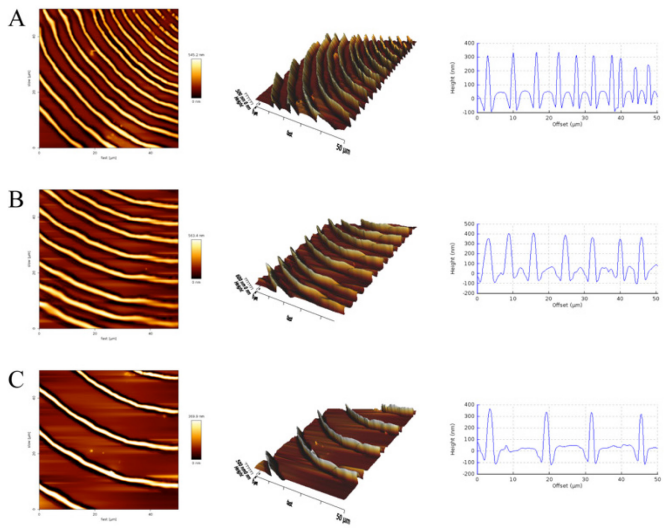

Figure 3.1 AFM image of ridges on pDR1m with Argon laser at 514 nm in 45 s: (left) bidimensional topographic image, (middle) 3D image and (right) cross section profile. Crest-to-crest distance: (A) 5 µm, (B) 10 µm and (C) 15 µm.

3.2.2 Real-Time Study of Cell Behavior

The peculiarity of the confocal technique is to produce dynamic topographic patterns whose features vary, in time and space, whit a high degree of resolution. This is of potential interest to study cell reaction and response to dynamically

evolving signals, more specifically, a topographic signal. Along this line, we evaluated how NIH-3T3 fibroblasts perceived these dynamic changes and thus modified their shape/orientation. Fibroblasts were stained with a vital stain Deep Red Cell Tracker TM in order to monitor the real-time changes in cell shape and position. The variations of the shape parameters were calculated every hour (up to a total of six hours) after pattern inscription. Flat polymeric films were used as control. Figure 3.2 shows a typical experiment in which a real-time analysis of cell behavior after inscription of different circular pattern is achieved in the presence of living cells. Interesting, fibroblasts seeded on imprinted circular patterns with 5 µm and 15 µm crest-to-crest groove distance did not perceive the pattern (Figure 3.2 A-C). Conversely, cells seeded on the circular pattern with 10 µm crest-to-crest groove distance displayed a stronger reaction to the underlying topography. In particular, after 2 hours fibroblasts started to align tangentially to the circumferential pattern and especially assumed circular disposition after 4-6 hours from inscription (Figure 3.2 B).

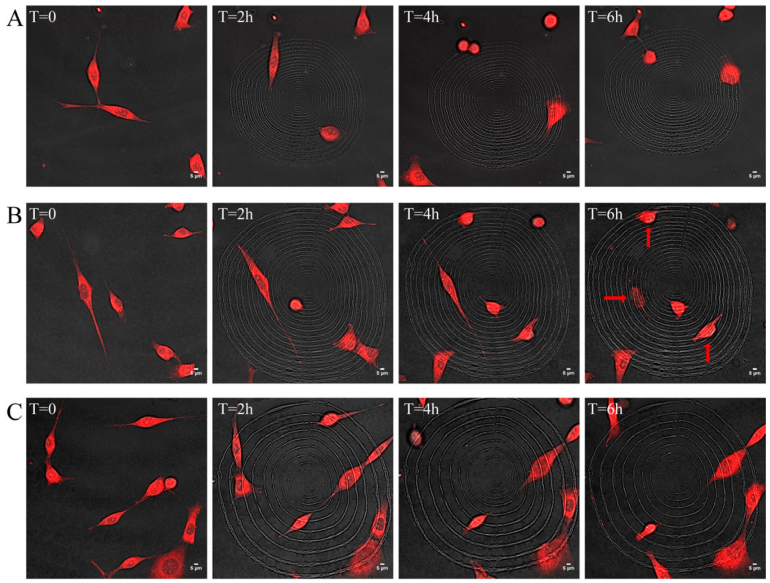

Figure 3.2 Cell behavior study on circular patterns in real-time. Confocal images of cells on different crest-to-crest groove distance (A) 5 µm, (B) 10 µm and (C) 15 µm. (T= 0) flat pDR1m, (T= 2, 4 and 6 h) same location after respectively 2, 4 and 6 hours after pattern inscription. Scale bars are 5 µm. Cells were stained with Deep Red. Red arrows indicate oriented cells.

Quantitative analyses were performed to estimate the cell behavior in terms of orientation, elongation over time (Figure 3.3). Regarding cell elongation, the principal moments of inertia (i.e., maximum and minimum) were evaluated to calculate the cell elongation index (Imax/Imin), which is an index of the shape anisotropy, i.e. if the index is close to 1 the shape is isotropic, whereas values greater than one are found for anisotropic and elongated cells. Cells did not show a strong tendency to elongate. After approximately 2 hours from the pattern inscription, NIH-3T3 fibroblasts, in contact with the pattern, showed an elongation with respect to the initial, non-patterned case. Conversely, cells showed a shortening approximately after 3 hours from the pattern inscription. Cell orientation on circular pattern was defined using the alpha angle (Figure 3.5). In this respect, we observed that fibroblasts on the 10 μm circular pattern showed a preferential direction of orientation. Particularly, starting from 4 hours after the pattern was embossed, the alpha angle decreased, so that cells aligned along the underlying pattern (Figure 3.3 B).

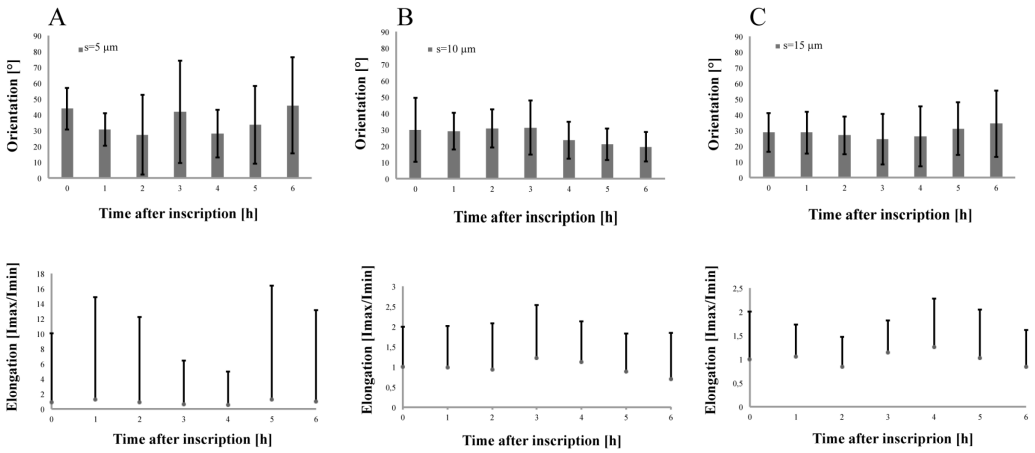

Figure 3.3 (Top set of graphs) Quantitative analysis of cell orientation on the different circular patterns. Crest-to-crest groove distance of (A) 5 μm (B) 10 μm and (C) 15 μm. (Bottom set of graphs) Quantitative analysis of cell elongation index on the different circular patterns. Crest-to-crest groove distance of (A) 5 μm (B) 10 μm and (C) 15 μm. Statistic on fifteen cells. Bars refer to the standard deviation.

Furthermore, fibroblasts on 5 μm and 15 μm circular pattern did not have a preferential direction of orientation during the entire experiment (average

orientation of ≈ 45°) (Figure 3.3 A-C). We hypothesized, that fibroblasts, on 5 µm circular pattern, reacted to the top of topographic features, while, on 15 µm crest-to-crest groove distance pattern, responded to the bottom part of topography. In these two types of circular topographies, cells perceived the patterned substrates as a flat azofilms and so presenting a random orientation.

3.2.3 Cell Mechanical Properties

Cell elasticity is a fundamental parameter that reflects the mechanical state of cells, which is related to the cytoskeleton assembly and contractility as well as to the membrane tension. The topographic features of material surfaces finely regulate cell fate and function via adhesion mediated signaling and cytoskeleton generated forces. However, how topography alters cell mechanic is still unclear. From literature, it is know that cell spreading and stiffness directly depend on underlying topography.[17] Consequently, topographic patterns might be used to induce specific cytoskeleton states. In our experiments, we evaluated cell property on circular pattern with respect to non-patterned case. Fibroblasts seeded on circular patterns whose groove distance was 10 µm tended to co-align with the underlying topography. The nucleus showed a relatively elongated shape, while the actin network did not show thick and mature stress fibers, which are normally observed on flat surfaces (Figure 3.4). Owing to these markedly different assemblies, it is reasonable to expect variations in the mechanical properties of cells. To evaluate the cell mechanical response to topographic features, we performed cell force mapping on cells cultivated on circular patterned (crest-to-crest groove distance of 10 µm) as well as on flat pDR1 substrates. We limited the analysis to this specific type of circular pattern, as it is the one that more effectively influenced cell orientation and cytoskeleton assemblies. Force mapping allowed us to calculate the mechanical properties of different cells, in terms of elastic or Young's modulus. Our data demonstrated that topographic patterns were recognized by cells and mechanical information was transferred by the cytoskeleton. Since actin network

predominantly dictates cell stiffness, AFM studies confirmed the observation of the immunofluorescence analysis. In fact, circular topographic pattern profoundly affected actin cytoskeleton assembly, also having an impact on cell mechanics. By AFM mechanical analysis, the average stiffness of fibroblasts seeded on the circular patterned sample was significantly lower when compared to the cell stiffness on un-patterned flat surfaces, and also the fibroblasts on circular pattern appeared much less elongated than cells seeded on flat substrates (Figure 3.4).

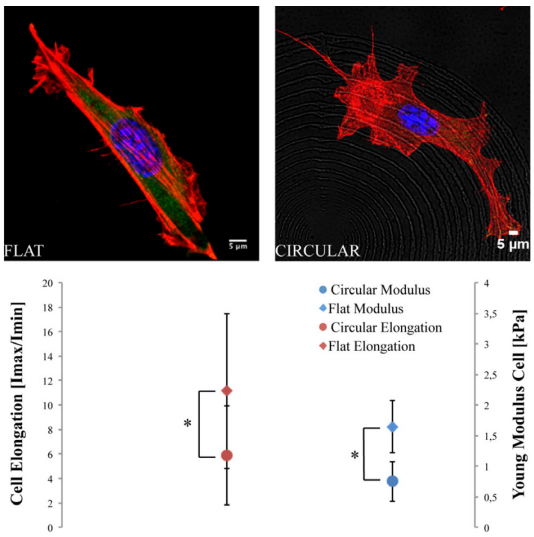

Figure 3.4 (Upper panel) Fluorescent images of fixed NIH-3T3 cells on flat film and circular patterns. Cell cytoskeleton is stained with phalloidin (red), focal adhesions are immunostained for vinculin (green) and nuclei are stained with draq5 (blue). Scale bars are 5 µm. (Lower panel) Quantitative analysis of mechanical property compared to cell elongation. Bars refer to the standard deviation. Data points referring to the value of modulus and elongation of cells seeded on flat and circular pattern are significantly different ($p < 0.05$).[10]

3.3 Conclusions

In this work, an innovative optical technique to emboss circular topographic patterns on azopolymer films has been presented, in order to study how the curvature of the topographic features could influence NIH-3T3 cell behavior. Recent discoveries confirmed that the curvatures guide some cell processes, not only in terms of adhesion and migration but also in terms of differentiation and

expression of carcinogenicity. In our experiments, several circular patterns were produced to evaluate the most appropriate dimensions perceived by cells. In detail, three different patterns were embossed by varying the crest-to-crest groove distance (5, 10, 15 μm.). Among these topographies, cells were strongly influenced by the pattern with 10 μm crest-to-crest groove distance. In fact, only in this case, cells responded to the underlying topography, they tended to align along the direction of pattern and to assume a circular disposition. Finally, we found that fibroblasts cultivated on patterned substrates possessed a significantly softer cell body and were less elongated with respect to cells on non-patterned substrates. These results were also confirmed by immunofluorescence images, in fact, on non-patterned films the actin network was more organized and the number of elongated fibroblasts was higher compared to the cells seeded on flat areas. Future developments will include the use of different cell lines, as for example stem cells, in order to study cell behavior not only in terms of cell elongation and orientation as shown in this study for fibroblasts, but also in terms of cell differentiation. All these experiments evidence the use of photosensitive azopolymer substrates, as a new kind of cell-instructive materials, for dynamic and programmable cell culture experiments in real-time.

3.4 Experimental Section

3.4.1 General Materials

Poly(Disperse Red 1 methacrylate) (pDR1m), all solvents, TRITC phalloidin were provided by Sigma. Cell Tracker Deep Red was supplied from Thermo Scientific, anti-vinculin monoclonal antibody was provided from Chemicon (EMD Millipore), Alexa Fluor 488 conjugated goat antimouse antibody and Deep Red Anthraquinone 5 (DRAQ-5) were purchased from Abcam. Fibroblast (NIH-3T3) cells were purchased from ATCC.

3.4.2 Sample Preparation

Spin coating technique was used to produce thin film of pDR1m on cover glasses. The solution was spun over the cover glass using a Laurell spin coater (Laurell Technologies Co.) at 1500 rpm. The film thickness was 300 nm, monitored using a profilometer.

3.4.3 Cell Culture

NIH-3T3 fibroblasts were cultured on azopolymer films. NIH-3T3 were cultured in low glucose DMEM (Dulbecco's Modified Eagle Medium) and incubated at 37 °C in a humidified atmosphere of 95% air and 5% CO_2. pDR1m substrates were sterilized under UV light for 30 min and subsequently cells were seeded on them without any additional treatment.

3.4.4 Pattern Fabrication

A SP5 laser scanning confocal microscope (Leica Microsystems, Germany) was used to emboss circular topographic patterns on pDR1m substrates using an Argon laser with 514 nm (maximum laser intensity of 2.6 mW) for 45 s.

3.4.5 AFM for Sample Surfaces Characterization

A JPK NanoWizard II (JPK Instruments, Germany) was used to assess information on the surface topography of pDR1m films. Silicon Nitride tips (MLCT, Bruker, USA), with a spring constant of 0.01 N/m, were used in contact mode, in air, at room temperature.

3.4.6 Dynamic Topographic Pattern Inscription

Fibroblasts were seeded on flat spin-coated film samples 24 hours prior to pattern inscription. Then, samples were attached with vacuum grease to the bottom of a fluoro-dish. Once at the microscope, a 40x/1.1 water immersion microscope objective was chosen as focusing lens. After focusing on the material surface, selected ROIs were drawn and the sample was irradiated at 514 nm Argon light for 45 s. Laser intensity was 1.3 mW and scan speed 400 Hz.

3.4.7 Live-Cell Staining and Immunofluorescence

Living cells were stained with Cell Tracker Deep Red. A stock solution of the dye was prepared in DMSO (10^3 μM), 2 μL of this solution was diluted with serum free medium (final volume of 1 mL). A SP5 confocal microscope was used to collect living cell images and videos. The dye was excited at 633 nm and emissions were collected in the range of 650-700 nm. In the case of cell immunofluorescence on patterned surfaces, after 24 h from cell seeding, cells were fixed with 4 % paraformaldehyde for 15 minutes and then permeabilized with 0.1 % Triton X-100 in PBS for 3 min. The actin filaments were stained with TRITC-phalloidin; samples were incubated for 30 min at room temperature in the phalloidin solution (dilution 1:200). For focal adhesions staining, cells were incubated in an anti-vinculin monoclonal antibody solution (dilution 1:200) for 2 h at 20 °C and successively marked with Alexa Fluor 488 conjugated goat anti-mouse antibody (dilution 1:1000) for 30 min at 20 °C. Finally cells were incubated for 15 min at 37 °C in a draq-5 solution (dilution 1:1000) to stain nuclei. The laser lines used were 488 nm (vinculin), 543 nm (actin) and 633 nm (nuclei). The emissions were collected in the ranges of 500-530, 560-610 and 650-720 nm, respectively.

3.4.8 Analysis of Cell Area, Orientation and Elongation

The qualitative study was evaluated on circular pattern embossed on cell-populated flat sample. The analyzed set of cells came from different experiments carried out in analogous conditions, considering different patterns inscribed in various regions of the azopolymer thin films sample. Morphometric analysis was performed using ImageJ software. Cell orientation on circular pattern was defined as the value of alpha angle. The alpha angle is the angle that the tangent to the circumference passing through the cell center forms with the cell axis. In detail, the value of alpha angle is calculated with the following equation:

$$\alpha = \theta - \phi \qquad \text{eq. 1}$$

where θ is the angle that the principal axis of inertia of the selected cell formed with the horizontal axis of the image and φ is the angle that the tangent to the circumference, passing through the center of the cell, formed with the horizontal axis (Figure 3.5).

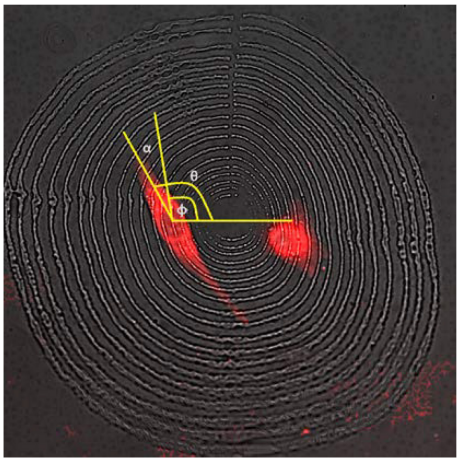

Figure 3.5. Graphic representation of the method for calculating the alpha angle.

Moreover, the principal moments of inertia (i.e., maximum and minimum) were evaluated and cell elongation index was defined as the ratio of the principal moments (Imax/Imin). High values of Imax/Imin identify elongated cells.

3.4.9 AFM for Cell Mechanics

A JPK NanoWizard II AFM was used to measure mechanical properties of living cells. An optical microscope was combined to the AFM to control tips and samples. Soft cantilevers (MLCT, Bruker, nominal spring constant 0.01 N/m) were used to investigate cell mechanical properties. For imaging the AFM was operated in contact mode at a scan rate of 1 line per second. During force mapping, spring constant of cantilever was first calibrated using a thermal tune method. Force curves were typically recorded at a scan rate of 1 Hz, corresponding to a maximum loading rate of 1 nN/s and a maximum force of 1 nN. Typically, 64 force curves were measured over a cell area of 3 x 3 μm. Mechanical properties of cells, in terms of Young modulus (E) values were estimated from each force curve within a force map. Evaluation was performed with the date analysis package IGOR (Wavemetrics). The Hertzian model was used to calculate Young's modulus for every force curve, thus 64 values were generated for each force map. The median was calculated from these values as a representative modulus of each force v. Statistical significance was assessed through t-test with level of significance $p < 0.05$.

3.5 References

1. Kilian, K. A.; Bugarija, B.; Lahn, B. T.; Mrksich, M., Geometric cues for directing the differentiation of mesenchymal stem cells. *Proceedings of the National Academy of Sciences* **2010,** *107* (11), 4872-4877.

2. Park, J. Y.; Lee, D. H.; Lee, E. J.; Lee, S.-H., Study of cellular behaviors on concave and convex microstructures fabricated from elastic PDMS membranes. *Lab on a Chip* **2009,** *9* (14), 2043-2049.

3. Li, Q.; Kumar, A.; Makhija, E.; Shivashankar, G., The regulation of dynamic mechanical coupling between actin cytoskeleton and nucleus by matrix geometry. *Biomaterials* **2014,** *35* (3), 961-969.

4. Rumpler, M.; Woesz, A.; Dunlop, J. W.; van Dongen, J. T.; Fratzl, P., The effect of geometry on three-dimensional tissue growth. *Journal of the Royal Society Interface* **2008,** *5* (27), 1173-1180.

5. Werner, M.; Blanquer, S. B.; Haimi, S. P.; Korus, G.; Dunlop, J. W.; Duda, G. N.; Grijpma, D.; Petersen, A., Surface curvature differentially regulates stem cell migration and differentiation via altered attachment morphology and nuclear deformation. *Advanced Science* **2017,** *4* (2).

6. Curtis, A.; Wilkinson, C., Topographical control of cells. *Biomaterials* **1997,** *18* (24), 1573-1583.

7. Flemming, R. G.; Murphy, C. J.; Abrams, G. A.; Goodman, S. L.; Nealey, P. F., Effects of synthetic micro- and nano-structured surfaces on cell behavior. *Biomaterials* **1999,** *20* (6), 573-88.

8. Bettinger, C. J.; Langer, R.; Borenstein, J. T., Engineering substrate topography at the micro-and nanoscale to control cell function. *Angewandte Chemie International Edition* **2009,** *48* (30), 5406-5415.

9. Schreiber, C.; Segerer, F. J.; Wagner, E.; Roidl, A.; Rädler, J. O., Ring-Shaped Microlanes and Chemical Barriers as a Platform for Probing Single-Cell Migration. *Scientific Reports* **2016,** *6*, 26858.

10. Rianna, C.; Rossano, L.; Kollarigowda, R. H.; Formiggini, F.; Cavalli, S.; Ventre, M.; Netti, P. A., Spatio-Temporal Control of Dynamic Topographic Patterns on Azopolymers for Cell Culture Applications. *Advanced Functional Materials* **2016,** *26* (42), 7572-7580.

11. Qi, L.; Li, N.; Huang, R.; Song, Q.; Wang, L.; Zhang, Q.; Su, R.; Kong, T.; Tang, M.; Cheng, G., The effects of topographical patterns and sizes on neural stem cell behavior. *PLoS One* **2013,** *8* (3), e59022.

12. Weigelin, B.; Friedl, P., Cancer cells: Stemness shaped by curvature. *Nature Materials* **2016,** *15* (8), 827.

13. Wang, K.; Cai, L.; Zhang, L.; Dong, J.; Wang, S., Biodegradable Photo-Crosslinked Polymer Substrates with Concentric Microgrooves for Regulating MC3T3-E1 Cell Behavior. *Advanced Healthcare Materials* **2012,** *1* (3), 292-301.

14. Lee, J.; Abdeen, A. A.; Wycislo, K. L.; Fan, T. M.; Kilian, K. A., Interfacial geometry dictates cancer cell tumorigenicity. *Nature Materials* **2016,** *15* (8), 856-862.

15. Zhang, Y.; Li, C.; Chan, V.; Kang, Y., Biomechanistic Study of Smooth Muscle Cell Sheet during Circumferential Alignment in Circular Micropatterns. *ACS Biomaterials Science & Engineering* **2015,** *1* (7), 549-558.

16. Jeng, R.; Chen, Y.; Kumar, J.; Tripathy, S., Novel crosslinked guest-host system with stable second-order nonlinearity. *Journal of Macromolecular Science—Pure and Applied Chemistry* **1992,** *29* (12), 1115-1127.

17. Yim, E. K.; Darling, E. M.; Kulangara, K.; Guilak, F.; Leong, K. W., Nanotopography-induced changes in focal adhesions, cytoskeletal organization, and mechanical properties of human mesenchymal stem cells. *Biomaterials* **2010,** *31* (6), 1299-1306.

Chapter 4

Dynamic Topographic Cues Modulate Cell Mechanical Properties, Focal Adhesion Remodeling and Cytoskeleton Organization.*

Abstract.

The influence of tunable topographic structures on cell behavior, in term of their effect provoked on cell adhesion, migration and polarization, has been examined and exploited. However, little is known about how these dynamic topographic cues could affect the mechanical properties of cells and subsequently cell functions in time. In this chapter, azobenzene-containing light-responsive biomaterials were employed as cell-instructive materials to induce dynamic topographic changes *in situ* during cell culture. The reported data demonstrate a time-dependent relationship between dynamic topographic cues and cell mechanical properties, cytoskeleton assembly and focal adhesion remodeling.

*The work described in this Chapter is a part of a manuscript in preparation. L. Rossano, M. Ventre, S. Cavalli and P. A. Netti: "Dynamic topographic cues modulate cell mechanical properties, focal adhesion remodeling and cytoskeleton organization".

4.1 Introduction

The role of the extracellular microenvironment in the regulation of many cell functions is well recognized and has been largely investigated. Indeed, it has been demonstrated that cell behavior is modulated via mechanical,[1] biochemical,[2] or topographical cues[3] and that cells rearrange, establish and break down extracellular components during cell physiological and pathological processes.[4] In particular, the extracellular environment exhibits rich topographies that interact directly with cells, generating a mutual dynamic interplay.[5] Recent findings showed that cells respond to dynamic topographic features on synthetic biomaterials.[6-7] Furthermore, several characteristics of cells can be largely influenced by the cell-material crosstalk. Among these, the mechanical properties of cells are dramatically affected by the cytoskeleton structure, its ability to generate forces along with focal adhesion (FA) mediated signaling which in turn are tightly connected to the topographic features of the culturing environment.[8-10] Several techniques are available to study cell mechanics, as for example micropipette aspiration,[11] optical stretcher[12] or atomic force microscopy (AFM).[13] In particular, AFM is suitable to study the mechanics of cells under physiological conditions, allowing elucidating the effects of substrate properties on cell behavior.[14] Nowadays, different reports concerning the influence of topographic cues on cell mechanics property and focal adhesion dynamics have been published.[15-16] For instance, it has been demonstrated that fibroblasts cultured on linear patterns possess significantly stiffer bodies and nuclei, in comparison to those cultured on flat substrates or grid patterns[4] and that the topographic properties of material surface can guide the focal adhesion remodeling.[17] However, an explanation of how tunable topographic cues could influence mechanical properties of cell and focal adhesion dynamics in time is missing. In order to fill this lack of knowledge the use of cell instructive materials, and in particular the use of light-responsive ones, might represent a new way of getting more insights in this field. Here we used Poly(Disperse Red 1 methacrylate)

(pDR1m) for its capability of changing its surface profile when irradiated with a focused laser beam of confocal microscope. This allowed modulating topographies on demand in order to evaluate the variation of NIH-3T3 mechanical properties in time and the remodeling of focal adhesions in a short period after the inscription of topographic features.

4.2 Results and Discussions

4.2.1 Mechanical Properties of Cells on Static Patterned Substrates.

AFM was used to investigate mechanical properties of NIH-3T3 cells subjected to different static topographic cues, based on the hypothesis that pattern mediated cell shape modulates cell stiffness and cytoskeletal stresses. To verify this, we performed cell force mapping on cells cultivated on flat as well as on patterned pDR1m substrates. Force mapping allowed us to calculate the mechanical properties of cells by fitting the force-indentation curves with a Hertzian model, which has been widely used to characterize cell mechanics.[18] Different types of gratings, linear, grid and circle patterns, were embossed on spin coated pDR1m films by using the confocal microscope technique, as previously described (Chapter 2). In detail, cell mechanical properties on flat, linear, grid and circle pattern were evaluated. These different topographic features were inscribed by using an Argon laser at 514 nm for 30 s (the intensity power was 1.3 mW). Flat azofilms were used as control surfaces. The Figure 4.1 shows the values of the Young's modulus on peripheral regions of fibroblasts after 24 h from seeding cells on several topographies.

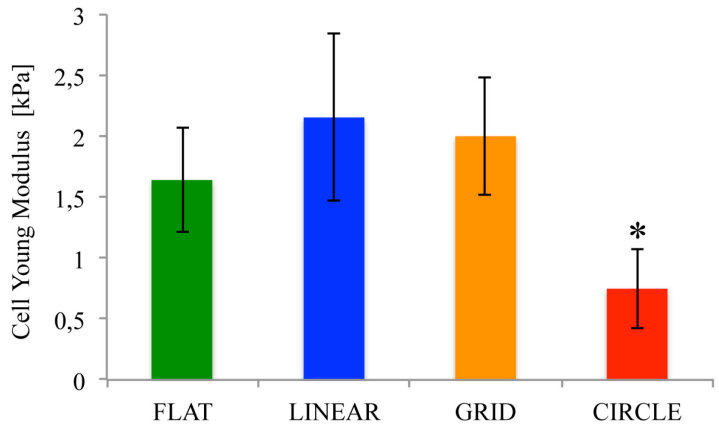

Figure 4.1 Young's modulus on peripheral regions of fibroblasts seeded on different topographies. Bars refer to the standard deviation. Data point referring to the circle case is significantly different than others ($p < 0.05$).

A strong dependence of cell elasticity to the geometry of underlying substrates was found. The fibroblasts cultivated on linear and grid patterned films possessed a significantly stiffer cell body. More specifically, the Young's modulus of cells on flat, linear and grid pattern was significantly higher than that of fibroblasts seeded on circle patterns. To better investigate the connections between topographic cues and cell response, immunofluorescence images were acquired. Confocal micrographs revealed several cytoskeletal structures that cells formed on the topographies, highlighting the influence of underlying pattern on cytoskeletal assemblies and cell mechanics. Fibroblasts on linear pattern were highly elongated, the majority of actin stress fibers was located along the length of the entire cell body and oriented to the same pattern direction. The nuclei were elliptical in shape (Figure 4.2 B). On flat and grid patterns (Figure 4.2 A-C), a network of thick assembled fibers was observed and the nuclei were spherical in shape. On circular pattern the nuclei showed an elliptical shape, the FAs grew in proximity of grooves with random orientation and the actin fibers were mostly limited to the cortical region (Figure 4.2 D).

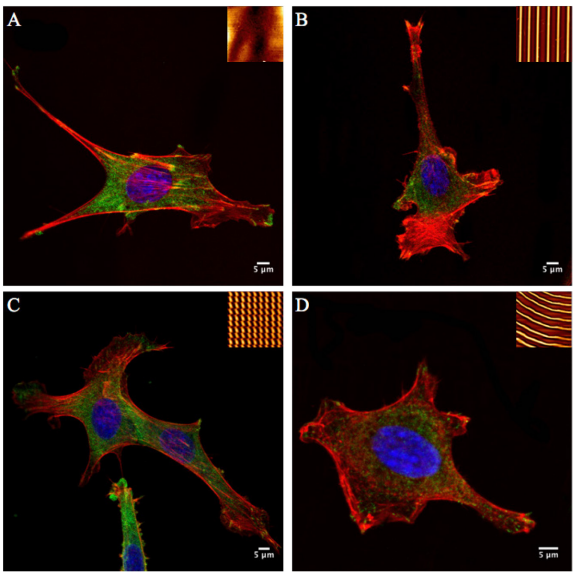

Figure 4.2. Confocal images of NIH-3T3 on (A) flat pDR1m (B) linear pattern (C) grid pattern and (D) circle pattern. The cell cytoskeleton is stained with phalloidin (red); FAs are immunostained for vinculin (green) and nuclei are stained with draq-5 (blue). 2D AFM images of the underlying topography are shown at the upper right corner of each confocal micrograph. Scale bars are 5 µm.

Our results provided further evidence of the role of topographic signals in affecting cell organization and mechanics. In detail, higher Young's moduli were observed in cells seeded on linear and grid topographies, where the actin fibers formed a dense and stable network. Conversely, the Young's modulus dramatically decreased when fibroblasts cells were cultured on circular pattern, indicating that a loss of actin filaments organization affected the cell mechanical stability.

4.2.2 Analysis of Cell Mechanical Properties on Dynamic Substrates.

Topographic features on pDR1 films in presence of live cells can be modulated in time and space using the confocal microscope technique. This allowed evaluating the modulation of cell mechanical property in response to the dynamic topographic cues. In detail, we calculated the Young's modulus of fibroblasts that reacted to the inscription of linear gratings (Figure 4.3). In the first case, in presence of live cells, a vertical linear pattern was embossed on flat azofilms, by irradiating the sample for 30 s using an Argon laser at 514 nm (laser intensity of 1.3 mW). In the second

case, using the same parameters for the inscription process, a horizontal pattern was embossed on the linear pattern itself eventually producing a grid.

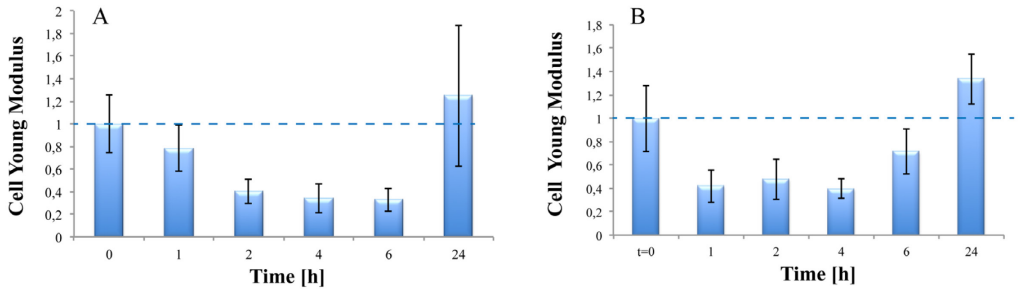

Figure 4.3 Variation of Young's modulus of cells in time subsequent to the pattern inscription process. (A) From flat to linear topography and (B) from linear to grid topography. Bars refer to the standard deviation. Variations are reported as fold changes with respect to the initial flat case t=0 (blue dashed line set at 1).

The previous data reported a decreasing of the Young's modulus of fibroblasts in the hours subsequent to the addition of topographic signals and an increase of this value the day after. In particular, after one hour form the inscription, cell body softening was greater for fibroblasts subjected to the transition from linear to grid topography (Figure 4.3 B) than for those cells subjected to the transition from flat to linear pattern (Figure 4.3 A). This difference could be explained presuming a different crosstalk between cells and flat or patterned substrates. On flat films, a stronger cell-material interaction, mediated by focal adhesion, could confirm the slower decrease of Young's modulus, which is consistent with literature data.[4] Instead, on patterned films, the topography reduced cell attachment, involving a faster cell cytoskeleton remodeling and a faster decrease of Young modulus. Since the inscription of topographic patterns profoundly affected the cell mechanics, it was expected that these cues also had an impact on cytoskeleton assembly.

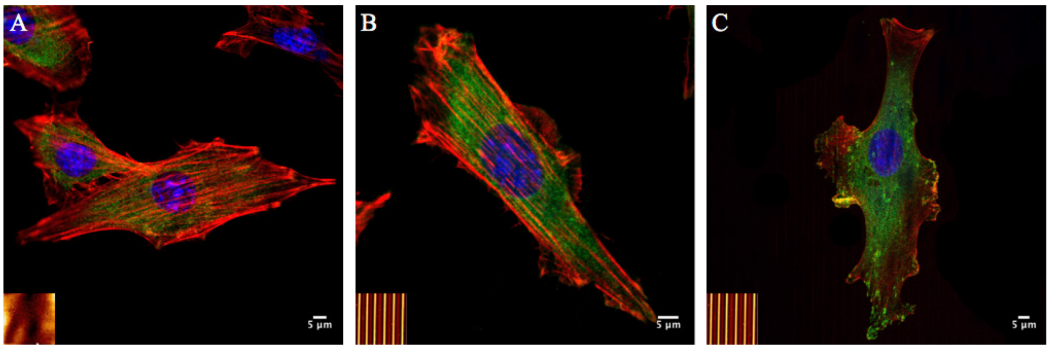

Figure 4.4. Confocal image of different NIH-3T3 cells on (A) flat pDR1m (B) linear pattern immediately after the inscription that corresponds to t=0 (C) linear pattern after 24 h from inscription. The cell cytoskeleton was stained with phalloidin (red), FAs were immunostained for vinculin (green) and nuclei were stained with draq-5 (blue). 2D AFM images of the underlying substrate are shown at the bottom left corner of each confocal micrograph. Scale bars are 5 µm.

The confocal images showed that fibroblasts on flat surfaces were randomly oriented and more defined stress fibers were observed in different directions (Figure 4.4 A). However, cells, after the inscription of linear pattern, exhibited mature F-actin aligned with its major axis (Figure 4.4 B). While, fibroblasts on linear patterns after 24 h were highly elongated and the majorities of stress fibers was oriented along the pattern direction. More intense spots of vinculin were observed at 24 h and at the end of actin fiber, which were assembled along the pattern direction (Figure 4.4 C). These experiments showed that, during the transition from linear to grid topography, a different cell response was observed.

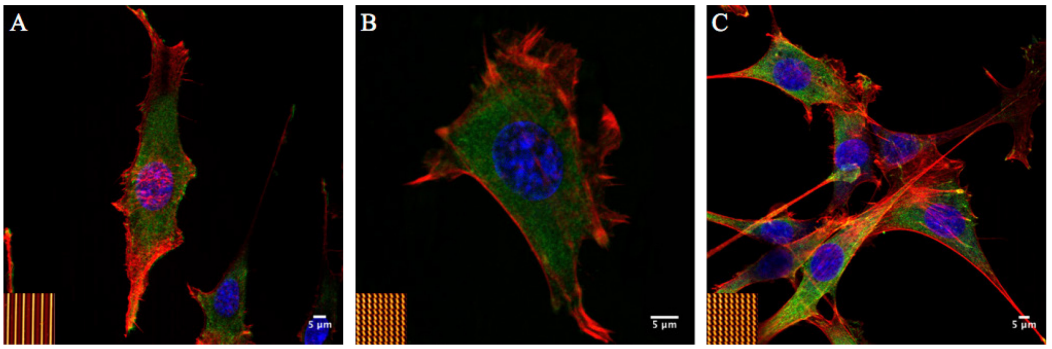

Figure 4.5 Confocal image of different NIH-3T3 cells on (A) linear pattern (B) grid pattern immediately after the inscription that corresponds to t=0 (C) grid pattern after 24 h from inscription. The cell cytoskeleton is stained with phalloidin (red); FAs are immunostained for vinculin (green), and nuclei are stained with draq-5 (blue). 2D AFM images of the underlying substrate are shown at the bottom left corner of each confocal micrograph. Scale bars are 5 µm.

Fibroblasts acquired an elongated morphology when they were seeded on the linear pattern (Figure 4.5 A). Immediately after the inscription of grid pattern, the formation of dense peripheral F-actin bundles appeared on the bordering region of the cell body (Figure 4.5 B), while a network of radially assembled fibers was observed on cells seeded on grid pattern (Figure 4.5 C). Finally, we measured the Young's modulus of fibroblast cells after the deletion of topographic signals (Figure 4.6). Linear gratings were irradiated using an incoherent and unpolarized light of mercury lamp for 45 s in order to remove the topographic signal.

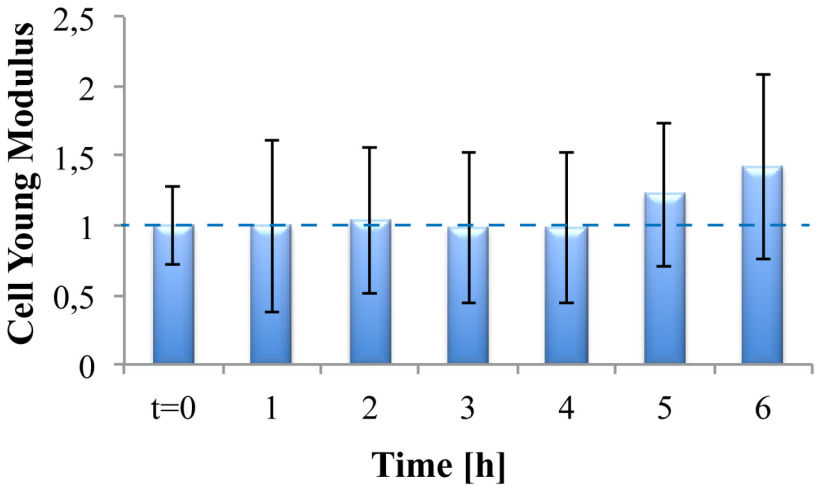

Figure 4.6 Variation of cell Young modulus in time subsequent to the deletion process. Bars refer to the standard deviation. Variations are reported as fold changes with respect to the initial flat case t=0 (blue line set at 1).

In this case, the Young 's modulus of fibroblasts did not change during the first four hours after the erase process and subsequently it started to increase. We hypothesized that fibroblasts did not perceive the deletion of pattern at short time, but they need to have a long period to reorganize them to the new topography. F-actin and focal adhesions were aligned parallel to the channel direction when fibroblasts were cultivated on linear pattern (Figure 4.7 A). After pattern erasing, the majority of focal adhesions appeared aligned parallel to the groove direction but the actin fibers were organized preferentially on the periphery of cell body (Figure 4.7 B). At 24 h from the erasure of linear pattern, fibroblasts were randomly

distributed; actin fibers and focal adhesions were oriented without any preferential alignment (Figure 4.7).

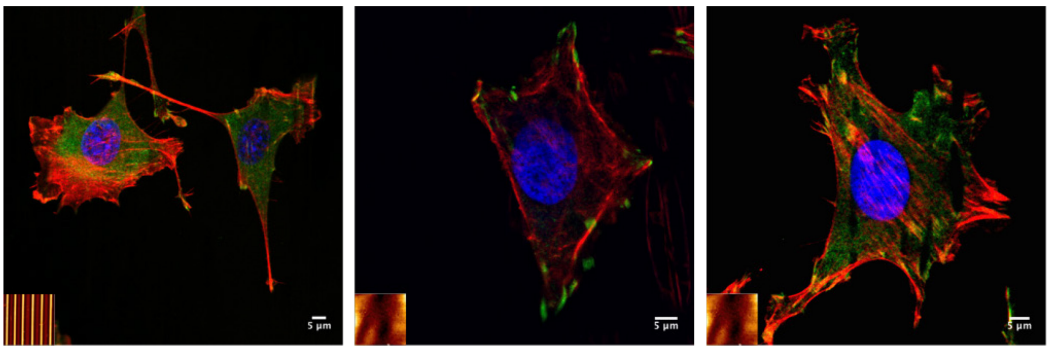

Figure 4.7 Confocal image of different NIH-3T3 cells on (A) linear pattern (B) erase pattern at t=0 (C) erase pattern after 24 h from deletion. The cell cytoskeleton is stained with phalloidin (red), FAs are immunostained for vinculin (green) and nuclei are stained with draq-5 (blue). 2D AFM images of the underlying substrate are shown at the bottom left corner of each confocal micrograph. Scale bars are 5 µm.

4.2.3 Investigation of Focal Adhesion Remodeling on Dynamic Surfaces.

Recent literature postulated that the material-cytoskeleton crosstalk and therefore cell-generated forces might be tuned via focal adhesion (FA) assembly.[16] Indeed, FAs play an important role in this process being the mechanical link between the cytoskeleton and the outside environment. Adhesions have often been presented as dynamic entities and their shape, dimension and spatial distribution change in according to the several cues acting on them. Similarly, the cytoskeleton changes its configuration according to the spatial arrangement and size of adhesions.[19] In our works, we focalized the attention on the influence of modular topographic cues on FA dynamics. Therefore, we limited to visualize and then analyze the geometrical features of FAs in the first hour subsequent to the inscription of a linear grating. Paxillin, a protein express in the FAs, was transfected with a plasmid bearing a fluorescence tag that could be detected at far-red wavelengths. The wavelength used for imaging (633 nm) do not overlap with the region of excitation of pDR1m. In this way, it was possible to analyze FA remodeling, influenced by topographic cues, in real-time without damaging the surface profile and/or interfering with the photopatterning process. The Figure 4.8 reports the values of

focal adhesion area and orientation for a single cell in time subsequent to the inscription of linear features. The measured angle was defined as the angle between the principal axis of FA and the horizontal axis. In detail, a cell-populated substrate was irradiated for 30 s using an Argon laser at 514 nm in order to emboss linear pattern.

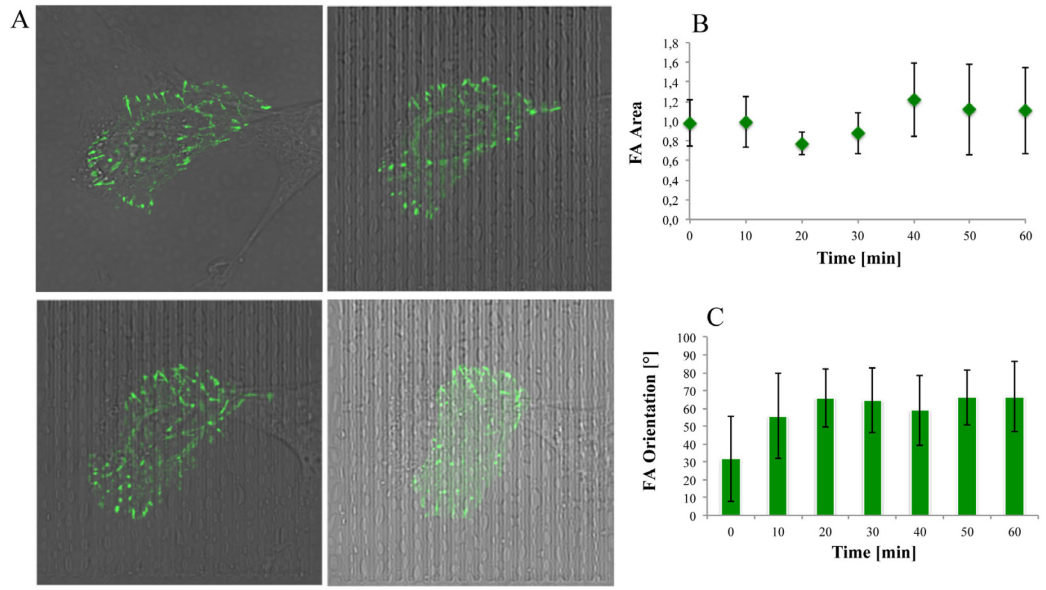

Figure 4.8 (A) FA alignment on pDR1m substrates in real-time. Cell was transfected with MKate2-Paxillin. Images were collected every 10 min after the liner pattern inscription. Scale bars are 5 µm. (B) Quantitative analysis of time-changes in FA area on the linear pattern. (C) Quantitative analysis of time-changes in FA orientation on the linear patterns. Bars refer to the standard deviation.

On flat surfaces, cell displayed FAs, which were randomly distributed. At longer time to the inscription of linear topography, FAs tended to orient towards the cell polarization axis. In detail, the FAs parallel to the linear pattern, did not change their direction and position in time, while FAs perpendicular to the topographies seemed to be “broken down” and migrated on the grooves and started to orient themselves already after 10 min from the pattern inscription. Concerning the orientation of the FAs polarization axis on flat film, we found that FAs were rotated of 31.79° (23.0° standard deviation) with respect to the horizontal direction. This value of orientation increased in time subsequent to pattern inscription (66.62° at 1 h), confirming the alignment of FAs with respect to the vertical pattern in time

(Figure 4.8 C). Instead, for this cell, the presence of the pattern did not affect FAs area at short time (Figure 4.8 B). We hypothesized that this specific geometric feature of FAs may take longer to change its value. In conclusion, focal adhesion assembly proved to be very sensitive to the underlying topographic signal, in fact, FAs reorganized their shape and orientation in response to dynamic topographic signals.

4.3 Conclusions

In this chapter, the influence of dynamic topographic cues on cell mechanical properties, focal adhesion remodeling and cytoskeleton organization was evaluated. The design of complex topographic features on biomaterials promotes focal adhesion growth and remodeling. In turn, this remodeling has a profound effect on the assembly of the cytoskeleton. The cytoskeleton organization regulates cell shape and polarization, which are crucial in the context of mechanotransduction. In detail, our data reported a decreasing of the Young modulus in the hours subsequent to the addition of topographic signals. On the contrary, an increasing of Young's modulus was observed the day after of the pattern inscription. Furthermore, the Young's modulus of fibroblasts did not change in response to the deletion of the linear pattern. It is known that the mechanical properties of the cell body, influenced by cytoskeleton organization, were also closely correlated to focal adhesion assembly. In fact, after the inscription of linear pattern, the fibroblast mechanical properties decreased and FAs reacted to the underlying topography, changing their orientation. These results demonstrated that the use of azofilms as dynamic cell-instructive materials paves the way to investigate cell behavior in a dynamic and biomimetic manner. To the best of our knowledge this is the first time that cell mechanical property, cytoskeleton and FA assembly can be investigated in real-time in response to dynamic topographic signals.

4.4 Experimental Section

4.4.1 General Materials

Poly(Disperse Red 1 methacrylate) (pDR1m), all solvents, TRITC phalloidin were provided by Sigma. Anti-vinculin monoclonal antibody was provided from Chemicon (EMD Millipore), Alexa Fluor 488 conjugated goat antimouse antibody and Deep Red Anthraquinone 5 (DRAQ-5) were purchased from Abcam. Fibroblast (NIH-3T3) cells were purchased from ATCC. mKate2-Paxillin was provided by Evrogen.

4.4.2 Sample Preparation

Spin coating technique was used to produce thin film of pDR1m on petri-dish. The solution was spun over the cover glass using a Laurell spin coater (Laurell Technologies Co.) at 1500 rpm. The film thickness was 300 nm, monitored using a profilometer.

4.4.3 Cell Culture

NIH-3T3 fibroblasts were cultured on azopolymer films. NIH-3T3 were cultured in high glucose DMEM (Dulbecco's Modified Eagle Medium) and incubated at 37 °C in a humidified atmosphere of 95 % air and 5% CO_2. pDR1m substrates were sterilized under UV light for 30 min and subsequently cells were seeded on them without any additional treatment.

4.4.4 Pattern Fabrication

A SP5 laser scanning confocal microscope (Leica Microsystems, Germany) was used to emboss linear topographic patterns on pDR1m substrates using an Argon laser with 514 nm (maximum laser intensity of 2.6 mW) for 30 s.

4.4.5 AFM for Sample Surfaces Characterization

A JPK NanoWizard II (JPK Instruments, Germany) was used to assess information on the surface topography of pDR1m films. Silicon Nitride tips (MLST, Bruker, USA), with a spring constant of 0.01 N/m, were used in contact mode, in air, at room temperature.

4.4.6 Dynamic Topographic Pattern Inscription

Fibroblasts were seeded on flat spin-coated film samples 24 hours prior to pattern inscription. Once at the microscope, a 40x/1.1 water immersion microscope objective was chosen as focusing lens. After focusing on the material surface, selected ROIs were drawn and the sample was irradiated at 514 nm Argon light for 30 s. Laser intensity was 1.3 mW and scan speed 400 Hz.

4.4.7 Immunofluorescence

Fibroblasts were fixed with 4% paraformaldehyde for 15 min and then permeabilized with 0.1% Triton X-100 in PBS for 3 min. The actin filaments were stained with TRITC-phalloidin; samples were incubated for 30 min at room temperature in the phalloidin solution (dilution 1:200). For focal adhesions staining, cells were incubated in an anti-vinculin monoclonal antibody solution (dilution 1:200) for 2 h at 20 °C and successively marked with Alexa Fluor 488 conjugated goat anti-mouse antibody (dilution 1:1000) for 30 min at 20 °C. Finally cells were incubated for 15 min at 37 °C in a DRAQ-5 solution (dilution 1:1000) to stain nuclei. The laser lines used were 488 nm (vinculin), 543 nm (actin) and 633 nm (nuclei). The emissions were collected in the ranges of 500-530, 560-610 or 650-720 nm, respectively.

4.4.8 AFM for Cell Mechanics

JPK NanoWizard II AFM was used to measure mechanical properties of living cells. An optical microscope was combined to the AFM to be able to control tips and samples. Soft cantilevers (MLCT, Bruker, nominal spring constant 0.01 N/m) were used to investigate cell mechanical properties. For imaging the AFM was operated in contact mode at a scan rate of 1 line per second. During force mapping, spring constant of cantilever was first calibrated using a thermal tune method. Force curves were typically recorded at a scan rate of 1 Hz, corresponding to a maximum loading rate of 1 nN/s and a maximum force of 1 nN. Typically, 64 force curves were measured over a cell area of 3 x 3 μm. Mechanical properties of cells, in terms of Young's modulus (E) values were estimated from each force curve within a force map. Evaluation was performed with the date analysis package IGOR (Wavemetrics). The Hertz model was used to calculate Young's modulus for every force curve, thus 64 values were generated for each force map. The median was calculated from these values as a representative modulus of each force v. Statistical significance was assessed through t-test with level of significance $p < 0.05$.

4.4.9 Live-Cell Confocal Microscopy

Fibroblast cells were seeded in 35 mm petri dish at 80% confluence and let overnight in incubator at 37 °C and 5% CO_2. Cells were then transfected with mKate2-Paxillin (Evrogen). The transfection complex was prepared in Opti-MEM I reduced serum medium (Gibco) and Lipofectamine 3000 (Invitrogen) was used as a transfection reagent. The amount of DNA/Lipofectamine was determined by following the supplier's instruction. Images were acquired with a Leica TCS SP5 equipped with heated sample holder environment (37 °C and 5 % CO_2) using a 40x/1.1 water immersion microscope objective. Preliminary experiments were

carried out to optimize confocal settings in order to minimize phototoxicity and photobleaching.

4.4.10 Analysis of Focal Adhesion Area and Orientation

Morphometric analysis (area, Feret length, orientation, major/minor axis aspect ratio) of focal adhesions was performed as follows. Digital images of FAs were firstly processed using blur command by following a modified procedure of the one proposed by Maruoka *et al*.[20] Blurred image were then subtracted from the original images using the image calculator command. The images were further processed with threshold command to obtain binarized images. Pixel noise was erased using the erode command and then particles analysis was performed in order to extract the morphometric descriptors. Only focal adhesions whose area was between 1.5 mm^2 and 5 mm^2 were included in the statistical analysis.

4.5 References

1. Yeung, T.; Georges, P. C.; Flanagan, L. A.; Marg, B.; Ortiz, M.; Funaki, M.; Zahir, N.; Ming, W.; Weaver, V.; Janmey, P. A., Effects of substrate stiffness on cell morphology, cytoskeletal structure, and adhesion. *Cytoskeleton* **2005,** *60* (1), 24-34.

2. van Kooten, T. G.; Spijker, H. T.; Busscher, H. J., Plasma-treated polystyrene surfaces: model surfaces for studying cell–biomaterial interactions. *Biomaterials* **2004,** *25* (10), 1735-1747.

3. Flemming, R.; Murphy, C.; Abrams, G.; Goodman, S.; Nealey, P., Effects of synthetic micro-and nano-structured surfaces on cell behavior. *Biomaterials* **1999,** *20* (6), 573-588.

4. Rianna, C.; Ventre, M.; Cavalli, S.; Radmacher, M.; Netti, P. A., Micropatterned azopolymer surfaces modulate cell mechanics and cytoskeleton structure. *ACS Applied Materials & Interfaces* **2015,** *7* (38), 21503-21510.

5. Smith, S. J., Neuronal cytomechanics: the actin-based motility of growth cones. *Science* **1988,** *242* (4879), 708-715.

6. Dalby, M. J.; Gadegaard, N.; Riehle, M. O.; Wilkinson, C. D.; Curtis, A. S., Investigating filopodia sensing using arrays of defined nano-pits down to 35 nm diameter in size. *The International Journal of Biochemistry & Cell Biology* **2004,** *36* (10), 2005-2015.

7. Bettinger, C. J.; Langer, R.; Borenstein, J. T., Engineering substrate topography at the micro-and nanoscale to control cell function. *Angewandte Chemie International Edition* **2009,** *48* (30), 5406-5415.

8. Moeendarbary, E.; Valon, L.; Fritzsche, M.; Harris, A. R.; Moulding, D. A.; Thrasher, A. J.; Stride, E.; Mahadevan, L.; Charras, G. T., The cytoplasm of living cells behaves as a poroelastic material. *Nature Materials* **2013,** *12* (3), 253.

9. Rotsch, C.; Radmacher, M., Drug-induced changes of cytoskeletal structure and mechanics in fibroblasts: an atomic force microscopy study. *Biophysical Journal* **2000,** *78* (1), 520-535.

10. McNamara, L. E.; McMurray, R. J.; Biggs, M. J.; Kantawong, F.; Oreffo, R. O.; Dalby, M. J., Nanotopographical control of stem cell differentiation. *Journal of Tissue Engineering* **2010,** *1* (1), 120623.

11. Lee, L. M.; Liu, A. P., The application of micropipette aspiration in molecular mechanics of single cells. *Journal of Nanotechnology in Engineering and Medicine* **2014,** *5* (4), 040902.

12. Guck, J.; Schinkinger, S.; Lincoln, B.; Wottawah, F.; Ebert, S.; Romeyke, M.; Lenz, D.; Erickson, H. M.; Ananthakrishnan, R.; Mitchell, D., Optical deformability as an inherent cell marker for testing malignant transformation and metastatic competence. *Biophysical Journal* **2005,** *88* (5), 3689-3698.

13. Radmacher, M.; Tillmann, R.; Fritz, M.; Gaub, H., From molecules to cells: imaging soft samples with the atomic force microscope. *Science* **1992,** *257* (5078), 1900-1906.

14. Rianna, C.; Kumar, P.; Radmacher, M. In *The Role of The Microenvironment in the Biophysics of Cancer*, Seminars in Cell & Developmental Biology, Elsevier: **2017.**

15. Yim, E. K.; Darling, E. M.; Kulangara, K.; Guilak, F.; Leong, K. W., Nanotopography-induced changes in focal adhesions, cytoskeletal organization, and mechanical properties of human mesenchymal stem cells. *Biomaterials* **2010,** *31* (6), 1299-1306.

16. Ventre, M.; Natale, C. F.; Rianna, C.; Netti, P. A., Topographic cell instructive patterns to control cell adhesion, polarization and migration. *Journal of the Royal Society Interface* **2014,** *11* (100), 20140687.

17. Diener, A.; Nebe, B.; Lüthen, F.; Becker, P.; Beck, U.; Neumann, H. G.; Rychly, J., Control of focal adhesion dynamics by material surface characteristics. *Biomaterials* **2005,** *26* (4), 383-392.

18. Radmacher, M.; Fritz, M.; Kacher, C. M.; Cleveland, J. P.; Hansma, P. K., Measuring the viscoelastic properties of human platelets with the atomic force microscope. *Biophysical Journal* **1996,** *70* (1), 556-567.

19. Goffin, J. M.; Pittet, P.; Csucs, G.; Lussi, J. W.; Meister, J.-J.; Hinz, B., Focal adhesion size controls tension-dependent recruitment of α-smooth muscle actin to stress fibers. *J Cell Biol* **2006,** *172* (2), 259-268.

20. Maruoka, M.; Sato, M.; Yuan, Y.; Ichiba, M.; Fujii, R.; Ogawa, T.; Ishida-Kitagawa, N.; Takeya, T.; Watanabe, N., Abi-1-bridged tyrosine phosphorylation of VASP by Abelson kinase impairs association of VASP to focal adhesions and regulates leukaemic cell adhesion. *Biochemical Journal* **2012,** *441* (3), 889-901.

Conclusions and Future Perspectives

The work described in this thesis aimed to propose a new class of cell-instructive materials fabricated to modulate their topographic features in a dynamic manner.

In vivo the extracellular matrix is an active network that continuously changes its biochemical and biophysical features. In detail, the ECM is a complex meshwork of pores, fibers, ridges, and other features of micro- or nano-meter size, which display dynamic topographic signals to cells. Currently, substrates with controlled topography have emerged as powerful tools in the investigation of the mechanisms involved in cell-topography crosstalk. The majority of these proposed substrates are intrinsically static in nature, thus, cannot be induce programmed changes of their surface properties. With such type of conventional systems, a thorough understanding of how cells integrate and respond to spatiotemporal changes of signals is impossible to achieve. For this reason, the development of systems able to change their surface properties in a controlled manner, directly in the presence of cells, is crucial to mimic the natural extracellular remodeling. However, most of these dynamic platforms are irreversible because they do not change their surface properties repeatedly. To enhance the versatility of these systems, thus enabling to investigate the cell response to dynamic topographic signals during culturing conditions, concepts such as precise spatio-temporal variations and reversibility of dynamic platforms need to be implemented. For this purpose, the confocal microscope set-up was used to pattern light-responsive surfaces with submicron scale resolution. In the field of light-responsive materials, azopolymers were used due to their capability to change their topographic feature in response to light stimuli. The topographic features can be embossed in an additive and sequential manner and eventually erased. The combination of confocal technique with the azopolymer surfaces seems to be a powerful tool to understand the cell-material crosstalk mechanisms.

In detail, in **Chapter 1** an introduction of azopolymers properties and of their

potential use as cell-instructive materials is given. Our attention has been focalized on the use of azopolymer surfaces as cell-instructive materials in order to present dynamic topographic cues to cells.

In **Chapter 2** an optical technique that allows the spatio-temporal modulation of topographic features on cell-populated surfaces is presented. The photopatterning of Poly(Disperse Red 1 methacrylate)-containing films (pDR1m) was obtained exploiting the linear polarization of the laser of the confocal microscope, while the deletion of the different topographic features, obtained with this technique, was produced using an incoherent and unpolarized light of mercury lamp mounted on the same set-up. Indeed, several patterns have been produced on cell-populated azopolymer films with fine control on time, space and on-off signal modification. In detail, we embossed linear grating with various pitch on azofilms in order to evaluate cell response in real-time. Initially, in static experiment, we demonstrated that epithelial cells responded to the underlying topography. Next, real-time inscription of a linear grating in the presence of living fibroblasts was achieved and analysis of cell behavior was conducted at single cell level. Importantly, the exposition to laser light did not affect cell viability and motility. Indeed, fibroblast cells reacted to such "dynamic" topographies, by modifying its morphology and orientation in time. Especially, after 5 h from pattern inscription, cells on the linear gratings were aligned along the groove direction.

In **Chapter 3** the fibroblasts response to modular circular topography, produced using the same confocal microscope technique, was examined. Recent investigations demonstrated that non-regular topography, presenting curvature, could influence cell behavior not only in terms of adhesion and migration but also in terms of differentiation and expression of carcinogenicity markers, promoting the opening of new avenues for cancer therapy. In this specific case, a real-time photopatterning of azofilms was conducted, revealing that fibroblasts could sense dynamic topographic changes and spontaneously adapted to a new environment by remodeling their cytoskeleton. As a matter of fact, on concentric circular pattern

with 10 μm crest-crest groove distance, fibroblasts tended to follow the underlying topographies. Furthermore, the Young's modulus of fibroblasts on such circle pattern was extremely low, indicating a poor organization of actin cytoskeleton on circular topographies that was confirmed by immunofluorescence imaging. These preliminary results represent a starting point for further studies on the effect of circular topographic signals on cell behavior.

Finally, in **Chapter 4** the investigation of complex cell processes involved in cell-topography interactions was reported in order to actively mimic *in vitro* what potentially happens *in vivo*. The real-time modulation of topographies embossed on cell-populated azofilms revealed a variation of Young's modulus of fibroblast cells and a remodeling of focal adhesions (FAs). In detail, the inscription of linear gratings caused a decreasing of Young's modulus and an orientation of FAs along the pattern direction, while the deletion of these topographies did not affect cell mechanical properties in the short time period after pattern inscription.

To the best of our knowledge, this innovative technique allowed for the first time, the evaluation of cell proprieties in response to the spatio-temporal manipulation of topographic cues. Taken together, these findings add a valuable contribution to actual application of azobenzene-based materials applied as light-responsive cell-instructive materials and, more specifically, as dynamic CIMs. Many times in this thesis, we have highlighted the potentialities of azobenzene-based materials and of the confocal microscope technique used for real-time photopatterning in providing the ideal tool for a precise spatio-temporal delivery of topographical signals to cells. The ability to modulate cues in presence of living cells is useful to answer specific questions concerning either fundamental study on cell–signal interactions or to deliberately affect cell fate. For example, to investigate on the time-variation of cell transcriptional activity in response to dynamically changing topographic signals or to evaluate which type of topographic features may influence stem cell differentiation at most.